MOLECULAR AND CELLULAR BIOLOGY, Apr. 2002, p. 2345–2365 Vol. 22, No. 7
0270-7306/02/$04.00+0 DOI: 10.1128/MCB.22.7.2345–2365.2002

RACK1, an Insulin-Like Growth Factor I (IGF-I) Receptor-Interacting Protein, Modulates IGF-I-Dependent Integrin Signaling and Promotes Cell Spreading and Contact with Extracellular Matrix

Ulrich Hermanto,[1] Cong S. Zong,[1] Weiqun Li,[2] and Lu-Hai Wang[1]*

Department of Microbiology, Mount Sinai School of Medicine, New York, New York 10029,[1] and Department of Oncology-Lombardi Cancer Center, Georgetown University Medical Center, Washington, D.C. 20007[2]

Received 19 November 2001/Returned for modification 7 December 2001/Accepted 27 December 2001

The insulin-like growth factor I (IGF-I) receptor (IGF-IR) is known to regulate a variety of cellular processes including cell proliferation, cell survival, cell differentiation, and cell transformation. IRS-1 and Shc, substrates of the IGF-IR, are known to mediate IGF-IR signaling pathways such as those of mitogen-activated protein kinase (MAPK) and phosphatidylinositol 3-kinase (PI3K), which are believed to play important roles in some of the IGF-IR-dependent biological functions. We used the cytoplasmic domain of IGF-IR in a yeast two-hybrid interaction trap to identify IGF-IR-interacting molecules that may potentially mediate IGF-IR-regulated functions. We identified RACK1, a WD repeat family member and a Gβ homologue, and demonstrated that RACK1 interacts with the IGF-IR but not with the closely related insulin receptor (IR). In several types of mammalian cells, RACK1 interacted with IGF-IR, protein kinase C, and β1 integrin in response to IGF-I and phorbol 12-myristate 13-acetate stimulation. Whereas most of RACK1 resides in the cytoskeletal compartment of the cytoplasm, transformation of fibroblasts and epithelial cells by v-Src, oncogenic IR or oncogenic IGF-IR, but not by Ros or Ras, resulted in a significantly increased association of RACK1 with the membrane. We examined the role of RACK1 in IGF-IR-mediated functions by stably overexpressing RACK1 in NIH 3T3 cells that expressed an elevated level of IGF-IR. RACK1 overexpression resulted in reduced IGF-I-induced cell growth in both anchorage-dependent and anchorage-independent conditions. Overexpression of RACK1 also led to enhanced cell spreading, increased stress fibers, and increased focal adhesions, which were accompanied by increased tyrosine phosphorylation of focal adhesion kinase and paxillin. While IGF-I-induced activation of IRS-1, Shc, PI3K, and MAPK pathways was unaffected, IGF-I-inducible β1 integrin-associated kinase activity and association of Crk with $p130^{CAS}$ were significantly inhibited by RACK1 overexpression. In RACK1-overexpressing cells, delayed cell cycle progression in G_1 or G_1/S was correlated with retinoblastoma protein hypophosphorylation, increased levels of $p21^{Cip1/WAF1}$ and $p27^{Kip1}$, and reduced IGF-I-inducible Cdk2 activity. Reduction of RACK1 protein expression by antisense oligonucleotides prevented cell spreading and suppressed IGF-I-dependent monolayer growth. Our data suggest that RACK1 is a novel IGF-IR signaling molecule that functions as a positive mediator of cell spreading and contact with extracellular matrix, possibly through a novel IGF-IR signaling pathway involving integrin and focal adhesion signaling molecules.

Insulin-like growth factor I (IGF-I) receptor (IGF-IR) is known to mediate a variety of cellular processes including cell proliferation, cell differentiation, cell transformation, and cell survival (22, 49, 51, 55). The major substrates recruited to IGF-IR after its activation are Shc and members of the insulin receptor substrate (IRS) family IRS-1 and IRS-2 (27, 58). Tyrosine-phosphorylated IRS-1 has been shown to associate with SH2 domain-containing molecules, including the protein tyrosine phosphatase Syp (SHP-2), the adapters Nck and Grb2, and the p85 regulatory subunit of phosphatidylinositol 3-kinase (PI3K) (42, 53, 57). Activation of PI3K and formation of its lipid products in vivo lead to activation of Akt/PKB and $p70^{S6}$ kinase, two downstream serine-threonine protein kinases involved in cell survival and protein synthesis pathways, respectively (8, 15, 18). Coupling of Grb2 to IGF-IR appears to occur through IRS-1 and Shc and leads to activation of Ras and the Raf/Mek/Erk kinase (mitogen-activated protein kinase [MAPK]) cascade via localization of the Grb2-Sos complex to the membrane-associated Ras. Activation of the Ras/MAPK pathway is known to mediate signaling leading to proliferation in many cell types, including NIH 3T3 fibroblasts (6, 10, 19). It is likely that molecules other than Shc and IRS proteins are involved in mediating signal transduction and functions of the IGF-IR. Recent studies on the identification of molecules that could serve as substrates for IGF-IR and/or interact with the receptor after its activation have revealed several additional potential downstream signaling molecules. These substrates include the guanine nucleotide exchange factors Vav (60) and Vav3 (66), the adapters CrkII and CrkL (4), and focal adhesion kinase (FAK) (3). Aside from IRS proteins, IGF-IR has been reported to interact in vitro and/or in vivo with numerous molecules, including the p85 subunit of PI3K (50, 59), Syp (50), GTPase-activating protein (50), the adapter Grb10 (37), C-terminal Src kinase (1), the scaffolding protein 14-3-3ε (17), and suppressor of cytokine signaling 2 (20). However, infor-

* Corresponding author. Mailing address: Department of Microbiology, One Gustave L. Levy Place, Box 1124, New York, NY 10029-6574. Phone: (212) 241-3795. Fax: (212) 534-1684. E-mail: lu-hai.wang@mssm.edu.

mation regarding the functional roles of many of these molecules in IGF-IR signaling and biological functions is currently limited.

While it has been shown that the protein tyrosine kinase FAK may function as a substrate for IGF-IR (3), its role in mediating integrin signaling is better understood (11). FAK becomes rapidly tyrosine phosphorylated after engagement of integrins with extracellular matrix (ECM) proteins or antibody (Ab)-induced clustering of integrins, leading to the formation of focal adhesion plaques, areas of the plasma membrane which make contact with and connect the actin cytoskeleton to the ECM (11). In addition to mediating cell adhesion with the ECM, integrins also function to regulate the reorganization of the cytoskeleton and the transduction of adhesion-dependent proliferative and survival signals. ECM- and integrin-initiated signals are mediated by focal adhesion protein complexes, which contain actin cytoskeleton-binding proteins, such as α-actinin, talin, tensin, vinculin, paxillin, and $p130^{CAS}$ and protein kinases such as FAK, protein kinase C (PKC), c-Src, and β1 integrin-linked kinase (ILK) (30). The activation of pathways mediated by ERK, c-Jun NH_2-terminal kinase (JNK), and ILK lead to the activation of transcription factors c-Fos, c-Jun, and β-catenin/TCF, respectively, and the subsequent induction of cyclin D1 expression and activation of cyclin-dependent kinase (Cdk) 4/6 activity, which are required for progression through the G_1 phase of the cell cycle (26). Cellular adhesion results in downregulation of the Cdk inhibitors (CKIs) $p21^{Cip1/WAF1}$ and $p27^{Kip1}$ and induction of cyclin E-Cdk2 activity, events necessary for transit through G_1 (26). The mechanism of integrin-mediated downregulation of $p21^{Cip1/WAF1}$ and $p27^{Kip1}$ is currently unknown. Adhesion-dependent signaling appears to be necessary for the optimal activation of the MAPK pathway by growth factor-dependent mitogenic signals (2). Additionally, growth factors such as IGF-I may cross-regulate integrin-dependent signaling pathways, since recent reports have demonstrated the tyrosine phosphorylation of paxillin and $p130^{CAS}$ and association of Crk with $p130^{CAS}$ after IGF-I stimulation (12, 24), but the significance of this cross-regulation remains unknown.

To identify signaling molecules that are involved in mediating IGF-IR-dependent functions, we used the cytoplasmic domain of IGF-IR as bait in a yeast two-hybrid interaction trap. We identified here an IGF-IR-interacting molecule called RACK1, which was originally named for its ability to bind to activated PKC in vitro (46). Subsequently, RACK1 was shown to interact with the cytoplasmic tail of β integrins after treatment with phorbol ester (33) and to interact with and inhibit the kinase activity of c-Src when overexpressed in NIH 3T3 cells (13), and this interaction was recently shown to be enhanced by activation of PKC and tyrosine phosphorylation of RACK1 (14). In addition, RACK1 was suggested to be an anchor for Ran1 (Pat1) kinase, a regulator for meiotic development in yeast (36). Very recently, RACK1 was shown to associate with PTPμ at cell-cell contacts (38) and to associate with the alpha interferon receptor and signal transducer and activator of transcription 1 (Stat1) to facilitate its activation (61).

In this study, we demonstrated the IGF-I-inducible intracellular interaction of RACK1 with IGF-IR, PKC, and β1 integrin. To address the role of RACK1 in IGF-IR-mediated functions, we introduced exogenous full-length RACK1 into an NIH 3T3 cell line that expressed an elevated level of IGF-IR (NIH 3T3-IGFR) and showed that overexpression of RACK1 resulted in the inhibition of IGF-I-dependent cell growth in both anchorage-dependent and anchorage-independent conditions. Overexpression of RACK1 altered the cell morphology of NIH 3T3-IGFR fibroblasts by enhancing the formation of stress fibers and focal adhesions concomitant with increased cell spreading, which were correlated with the increased tyrosine phosphorylation of FAK and paxillin. The major IGF-IR mitogenic signaling pathways mediated by IRS-1, Shc, PI3K, and MAPK were unaffected. In contrast, IGF-I-inducible signaling by β1 integrin and focal adhesion molecules, including $p130^{CAS}$, paxillin, and Crk, was perturbed in these cells. RACK1 overexpression, with resultant cell cycle delay in G_1 or G_1/S, was correlated with increased levels of $p21^{Cip1/WAF1}$ and $p27^{Kip1}$ and reduced IGF-I-dependent cyclin E-associated kinase activity. Introduction of antisense oligonucleotides into Swiss 3T3 cells reduced RACK1 expression, inhibited cell spreading, and suppressed IGF-I-dependent monolayer cell proliferation. This report provides initial evidence for a role of RACK1, a novel IGF-IR-interacting molecule, in the regulation of focal adhesion-based cytoskeletal reorganization and IGF-I-dependent cell growth, cell transformation, and integrin-mediated signaling.

MATERIALS AND METHODS

Yeast two-hybrid interaction trap. The LexA-based yeast two-hybrid interaction trap was used it to identify potential IGF-IR-interacting proteins (23, 67) as we had previously used to identify IR-interacting proteins (16). A fragment of IGF-IR containing the entire cytoplasmic domain was generated by PCR with primers 5′-ATCCGTCGACCAAGAAAGAGAAATAAC-3′ and 5′-GCAGGT CGACTCATCCAAGGATCAGCA-3′, which contain *Sal*I sites for in-frame cloning into bait plasmid pEG202. *Sal*I digestion and ligation were performed to generate pEG202-IGFR, and the IGF-IR sequence was verified by dideoxy sequencing with the Sequenase DNA sequencing kit (U.S. Biochemicals). Protein expression of the bait and its in vitro and in vivo PTK activity were confirmed (data not shown). Standard yeast two-hybrid procedures were used to transform EGY48 yeast with bait plasmid, pSH18-34 reporter plasmid, and a human (HeLa cell) cDNA library (pJG4-5) to screen for clones which conferred β-galactosidase activity and the ability to grow on nutrient selection plates lacking leucine. A 1.1-kb cDNA insert from one of the positive clones was subcloned into pBluescript (Stratagene) with *Eco*RI and *Xho*I and sequenced bidirectionally by the dideoxy method with primers complementary to sequences 5′ and 3′ to the cloning sites of pJG4-5. The complete sequence was compared to sequences in GenBank with BLASTN and BLASTX search algorithms and was found to encode full-length RACK1. To confirm and compare bait-prey interaction, yeast cells containing bait pEG202-IGFR or pEG202-IR-L, encoding the kinase active cytoplasmic domain of IR (16), were transformed with pJG4-5 library plasmids encoding RACK1, Stat5b, or the empty vector.

Mammalian expression plasmids. Primers 5′-GCTGGTACCGAGGCACGA GGCGGCGTG-3′ (sense [primer 1]), 5′-TGCTCTAGACTTCTAGCGTGTGC CAAT-3′ (antisense [primer 2]), 5′-CCCAAGCTTACCATGGACTACCCTTA TG-3′ (sense primer with hemagglutinin [HA] sequence [primer 3]), and 5′-AC ATGCATCTAGGCATAATCTGGCACATCATAAGGGTATGCGCCATCT GCGCCGCGTGTGCCAATGGTCACCTG-3′ (antisense primer with HA sequence [primer 4]) and the template pJG4-5-RACK1 were used to generate RACK1 PCR fragments containing an HA epitope sequence at either the 3′ end (primer pair 1 and 4) or the 5′ end (primer pair 2 and 3). The PCR-generated fragments were cloned into the mammalian expression vector phEF-Neo, a plasmid containing the human elongation factor 1 promoter and the neomycin resistance gene, to generate phEF-HA-RACK1 (5′ HA) and phEF-RACK1-HA (3′ HA). The phEF-RACK1 plasmid, encoding full-length RACK1, was generated by combining a fragment of phEF-RACK1-HA containing the 5′ RACK1 sequence with a fragment of phEF-HA-RACK1 containing the remaining 3′ RACK1 sequence, which effectively eliminated the HA sequence. All constructs

were verified by dideoxy sequencing. The IGF-IR expression plasmids, pMX-IGFR, and phEF-IGFR have been described previously (34, 68).

Cell culture. Cells were maintained at 37°C and 5% CO_2 in a humidified incubator except where noted. Swiss 3T3, NIH 3T3, R2-IGFR, NIH 3T3-IGFR, 3T3-RasV12, rat intestinal epithelial (RIE)-NM1, RIE-T6, and 3Y1-Src cells were grown in Dulbecco's modified Eagle medium (DMEM; Gibco) supplemented with 5% heat-inactivated bovine calf serum (BCS; Gibco) and routinely used antibiotics. Human embryonic kidney (HEK) 293T epithelial cells were grown in the same conditions as described above except with 10% heat-inactivated fetal bovine serum (FBS; Gibco). Primary chicken embryo fibroblasts (CEF) and virus-infected CEF were grown in DMEM containing 5% heat-inactivated BCS and 1% heat-inactivated chicken serum and antibiotics. NIH 3T3-IGFR and R2-IGFR cells, which stably overexpress IGF-IR, were generated by transfection of NIH 3T3 and Rat2 fibroblasts with pMX-IGFR (encodes the full-length human IGF-IR under the control of the Moloney murine leukemia virus long terminal repeat) by the calcium phosphate method and subsequent selection with neomycin. The generation of RIE-NM1 and RIE-T6 cells, which are rat intestinal epithelial cells stably expressing NM1 and T6, oncogenic gag-human IGF-IR and gag-human IR fusion receptors, respectively, was described previously (40). 3Y1-Src rat fibroblasts, which express v-Src, were generated previously in our laboratory by infection of 3Y1 cells with SR-A Rous sarcoma virus and clonal selection. 3T3-RasV12, an NIH 3T3 cell line expressing an activated H-Ras mutant, was kindly provided by Andrew Chan at Mount Sinai School of Medicine.

DNA transfection and generation of stable NIH 3T3-IGFR/RACK1 cell lines. Transfections were performed by the method of calcium phosphate coprecipitation as described previously (68). HEK293T cells were grown to 50% confluence and transfected with 10 μg of phEF-IGFR alone or cotransfected with 5 μg of phEF-IGFR and 5 μg of phEF-Neo, phEF-RACK1, phEF-HA-RACK1, or phEF-RACK1-HA for 12 to 16 h. Cells were allowed to recover for 24 h in fresh medium before serum starvation and treatment with IGF-I or phorbol 12-myristate 13-acetate (PMA). NIH 3T3-IGFR cells were plated at a density of 5×10^5/10-cm dish and were cotransfected with 10 μg of phEF-RACK1-HA or phEF-Neo and 1 μg of pBabePuro, a murine retrovirus long terminal repeat-based plasmid containing the puromycin resistance gene. Drug-resistant transfectants were selected in medium containing 5 μg of puromycin (Sigma)/ml beginning 24 h after transfection. Individual colonies were isolated and amplified as individual clones, and the remaining colonies were pooled and amplified as a mass culture.

Infections. Stock supernatants containing viruses encoding gag-IGFR (NM1), v-Ros (UR2), and v-Src (SR-A), as well as temperature-sensitive (*ts*) mutants of gag-IGFR (*ts*NM1), v-Ros (*ts*ROS), and v-Src (*ts*Src), were generated previously in this laboratory. Early passage primary CEF were infected with an aliquot of a given virus stock in the presence of 2 μg of Polybrene/ml. Infected CEF were maintained at 37°C prior to experiments. Cells that were infected with *ts* mutants were incubated at 41°C (the nonpermissive temperature) for 3 days before being shifted to 35°C (the permissive temperature) for the times indicated in the figure legends. Subcellular fractionation and protein analyses were subsequently performed. Oncogenic transformation, marked by distinct and characteristic morphologic changes of CEF, was typically evident 24 to 48 h after the shift to a permissive temperature.

Morpholino oligonucleotides. Morpholino oligonucleotides of the murine RACK1 sequence were generated by Gene Tools. The sequence of the antisense oligonucleotide is 5′-CACGAAGGGTCATTTGCTCGGTCAT-3′ and that of the standard control oligonucleotide is 5′-CCTCTTACCTCAGTTACAATTTA TA-3′. The manufacturer's protocol was used to deliver the morpholino oligonucleotides. Briefly, 3×10^5 trypsinized Swiss 3T3 cells were seeded into each well of a six-well culture plate 1 day prior to delivery. On the following day, the medium in each well was replaced with 1 ml of fresh medium. Antisense or control morpholino oligonucleotides were added to a final concentration of 10 μM and swirled for 10 s. Cells were then gently scraped off the surface of the well, pipetted up and down, and transferred to a new culture plate, and this process was repeated 4 h later. Cells were then maintained in culture for subsequent experiments.

Abs. Anti-RACK1, anti-PKCδ, anti-PKCμ, anti-FAK (for immunoblotting [IB]), anti-paxillin, anti-$p130^{CAS}$, anti-Crk, anti-Shc, anti-phosphotyrosine-horseradish peroxidase (RC20-HRP), anti-mouse immunoglobulin G (IgG)-HRP, and anti-rabbit IgG-HRP Abs were purchased from Transduction Laboratories. Anti-$p21^{Cip1}$, anti-$p27^{Kip1}$, anti-Cdk4, anti-Cdk6, anti-Cdk2, anti-cyclin D1, anti-cyclin E, and anti-cyclin A Abs were purchased from Santa Cruz Biotechnology. Anti-phospho-Akt (Ser473), anti-phospho-p70S6 kinase (Ser411), and anti-phospho-ERK1/2 (Thr202/Tyr204) Abs were purchased from New England Biolabs. Anti-$p85^{PI3K}$ and anti-FAK (for immunoprecipitation) Abs were purchased from Upstate Biotechnology, Inc. Anti-β1 integrin Ab was purchased from Gibco. Anti-IGFRα (extracellular domain) Ab was purchased from Calbiochem. Anti-GAPDH (glyceraldehyde-3-phosphate dehydrogenase) Ab was purchased from Biodesign International. Anti-vinculin Ab, phalloidin-fluorescein isothiocyanate (FITC), and phalloidin-tetramethyl rhodamine isothiocyanate (TRITC) were purchased from Sigma. Anti-retinoblastoma (Rb) Ab was purchased from PharMingen. Anti-mouse IgG-FITC and anti-rabbit IgG-FITC Abs were purchased from Boehringer Mannheim. Abs were used according to the manufacturer's recommended dilutions unless otherwise noted. Anti-mouse IgG and anti-mouse IgM secondary Abs for immunoprecipitation were purchased from Accurate. Anti-IGFR (cytoplasmic domain) and anti-IRS-1 Abs were described previously (34, 69) and were used at 1:500 and 1:250 dilutions, respectively.

Stimulation of cells. Cells grown to confluence or after transfection (HEK293T) were incubated in serum-free DMEM. After 24 h, the cells were incubated in serum-free DMEM supplemented with 100 ng of IGF-I (Intergen) per ml, 0.2 μM PMA (Sigma), or 5% BCS for 2, 5, 10, 20, 30, or 50 min as indicated in the figure legends. Cells were then immediately placed on ice. Unstimulated control cells were mock treated with serum-free DMEM for 10 min.

Preparation of cell lysates and immunoprecipitates. Cells were placed on ice and were washed twice with cold Tris-Glu buffer (25 mM Tris-HCl, pH 7.4; 150 mM NaCl; 5 mM KCl; 1 mM sodium phosphate; 0.1% glucose). For protein analysis, cells were lysed with radioimmunoprecipitation assay (RIPA) buffer (50 mM Tris-HCl, pH 7.4; 150 mM NaCl; 1% deoxycholate; 1% Triton X-100; 5 mM EDTA; 1% aprotinin; 1 mM sodium orthovanadate; 0.4 mM phenylarsine oxide [PAO]) for immunoprecipitation or with Western lysis buffer (10 mM Tris-HCl, pH 7.4; 1% sodium dodecyl sulfate [SDS], 1 mM phenylmethylsulfonylfluoride [PMSF]; 1% aprotinin; 1 mM sodium orthovanadate; 0.4 mM PAO; 25 mM NaF) for direct Western analysis. For coimmunoprecipitation, cells were permeabilized for a minimum of 30 min with one of three solutions, namely, digitonin buffer (1% digitonin [Boehringer Mannheim]; 150 mM NaCl; 20 mM Tris-HCl, pH 7.4; 1 mM PMSF; 1% aprotinin; 1 mM sodium orthovanadate; 0.4 mM PAO; 25 mM NaF; 5 mM EDTA), NP-40 buffer (1 or 0.5% NP-40; 20 mM Tris-HCl, pH 7.4; 150 mM NaCl; 5 mM EDTA; 1 mM PMSF; 1% aprotinin; 1 mM sodium orthovanadate), or CHAPS {3-[(3-cholamidopropyl)-dimethylammonio]-1-propanesulfonate} buffer (10 mM CHAPS Σ; 50 mM Tris-HCl, pH 8.0; 150 mM NaCl; 2 mM EDTA; 1 mM PMSF; 1% aprotinin; 1 mM sodium orthovanadate; 15 mM NaF; 10 mM sodium pyrophosphate) as indicated in the figure legends. Cell lysates were clarified by centrifugation at 12,000 rpm for 10 min at 4°C. Protein concentration of the supernatants were determined by Bradford assay, and equivalent amounts of protein from cell lysates were used for immunoprecipitation or analyzed directly by SDS-polyacrylamide gel electrophoresis (PAGE) followed by Western blotting. For immunoprecipitations, the indicated Ab was added to lysates and allowed to rock at 4°C for 2 to 4 h (kinase assays) or overnight (others). Then, 1 μg of anti-mouse IgG Ab (for monoclonal primary Abs) or anti-mouse IgM Ab (for anti-RACK1 Ab) and 25 μl of protein A-Sepharose beads (Repligen) were added to the lysates, which were allowed to rock for another 2 h at 4°C. Immunoprecipitates were washed twice by gentle vortexing in fresh cold RIPA buffer (for protein analysis), 0.2% digitonin buffer (for digitonin-permeabilized lysates), or 0.5% NP-40 buffer (for NP-40-permeabilized lysates). Washed immunoprecipitates and total cell lysates were denatured by boiling after the addition of one-sixth of the volume of 6× reducing SDS-PAGE sample buffer (360 mM Tris, pH 6.6; 12% SDS; 600 mM dithiothreitol [DTT]; 60% glycerol; 0.6% bromophenol blue) and analyzed by SDS-PAGE and immunoblotting.

In vitro kinase assays. (i) Integrin-associated kinase assay. Anti-β1 integrin immunoprecipitates were washed once in CHAPS buffer, twice in HBS (20 mM HEPES, pH 7.4; 150 mM NaCl), and twice in kinase buffer (50 mM HEPES, pH 7.0; 10 mM $MnCl_2$; 10 mM $MgCl_2$; 2 mM NaF; 1 mM sodium orthovanadate). Immunoprecipitates were resuspended in 30 μl of kinase buffer, and reactions were initiated by addition of 1 μl (10 μCi) of [γ-^{32}P]ATP and incubated at 30°C for 20 min. Reactions were terminated by the addition of 10 μl of 6× SDS-PAGE sample buffer and boiling for 5 min. The supernatants were resolved by SDS–10% PAGE and electroblotted to nitrocellulose filters according to standard protocols. Phosphorylated proteins were detected by exposure of membranes to Kodak XAR-5 film at −70°C for appropriate times.

(ii) IRS-1-associated PI3K assay. Anti-IRS-1 immunoprecipitates were assayed for in vitro PI3K activity by using [γ-^{32}P]ATP and phosphatidylinositol (Avanti Polar Lipids) as substrates, as described previously (34). Phosphorylated products were separated on Silica Gel 60 TLC plates (Merck) and detected by autoradiography.

(iii) Cdk assay. Cells were lysed in a lysis buffer containing 50 mM HEPES (pH 7.4), 50 mM NaCl, 0.5% Triton X-100, 1 mM DTT, 20 mM NaF, 10 mM

$NaPP_i$, 400 μM PAO, 1 mM sodium vanadate, 1% aprotinin, and 5 μg of leupeptin/ml. Then 200 μg of total cellular protein was immunoprecipitated with anti-cyclinE Ab for 16 h at 4°C, followed by the addition of protein A-Sepharose beads and further incubation for 1 h. Beads were collected by centrifugation, washed twice in lysis buffer without protease and phosphatase inhibitors, and washed once in kinase reaction buffer (50 mM HEPES, pH 7.4; 10 mM $MgCl_2$). Immunoprecipitates were resuspended in 40 μl of kinase reaction buffer supplemented with 50 μM ATP, 1 μg of histone H1, and 0.7 μCi of [γ-^{32}P]ATP and then incubated for 20 min at 30°C. The reaction was terminated by boiling after the addition of the appropriate volume of 6× SDS loading buffer, and the supernatant was analyzed as described above for integrin-associated kinase assay.

SDS-PAGE and immunoblotting. Protein samples were fractionated on SDS-polyacrylamide gels and electroblotted onto nitrocellulose membranes according to standard protocols. The membrane was blocked by incubating in TBS-Tween (10 mM Tris-HCl, pH 7.4; 50 mM NaCl; 0.1% Tween 20) containing 5% (wt/vol) nonfat dry milk or 3% (wt/vol) BSA (for RC20-HRP) and sequentially incubated with the indicated primary Ab and a HRP-conjugated secondary anti-mouse or anti-rabbit Ab (depending on the primary Ab). Membranes were then washed with TBS-Tween and developed by the enhanced chemiluminescence method according to the manufacturer's instructions (Amersham). Where indicated, the membrane was stripped of Ab by three washes with glycine buffer (0.2 M glycine, pH 2.0) and three washes with TBS-Tween and then immunoblotted with the indicated Ab.

Subcellular fractionation. (i) S100/P100 fractionation. Cells were placed on ice and washed twice with Tris-Glu buffer. Cells were then collected in Tris-Glu buffer and centrifuged at 1,500 rpm for 5 min at 4°C. Cells were then resuspended in a hypotonic buffer (20 mM Tris-HCl, pH 7.4; 10 mM KCl; 1 mM EDTA; 1 mM DTT; 1% aprotinin; 1 mM PMSF) and kept on ice for 10 min. The cells were Dounce homogenized with a type B pestle (20 to 40 strokes) until >90% of the cells were broken and the release of nuclei was confirmed by examination under a microscope. The cell suspension was adjusted with NaCl to 125 mM. The cell lysate was then centrifuged at 1,500 rpm for 10 min to pellet the nuclei and cell debris (P1 fraction), and the supernatant was collected and further centrifuged at 100,000 × *g* in polycarbonate tubes for 30 min at 4°C. The supernatant (S100 fraction), containing cytosolic components, was removed and adjusted to 1% Triton X-100. The pellet (P100 fraction), containing cellular membrane components, was solubilized in RIPA buffer containing 0.1% SDS and then centrifuged at 12,000 rpm for 10 min at 4°C to generate the soluble P100 fraction (supernatant). The S100 and soluble P100 fractions were analyzed by immunoprecipitation, SDS-PAGE, and immunoblotting.

(ii) CSK fractionation. Cells were placed on ice, washed twice with Tris-Glu buffer, and gently incubated in 0.5 ml of CSK buffer (1% Triton X-100; 10 mM PIPES [piperazine-*N*,*N*′-bis(2-ethanesulfonic acid)], pH 6.8; 100 mM KCl; 2.5 mM $MgCl_2$; 1 mM $CaCl_2$; 300 mM sucrose; 1 mM PMSF; 1% aprotinin; 1 mM sodium orthovanadate) for 3 to 5 min. The buffer was collected with minimal perturbation of the cell monolayer. Another 0.5 ml of CSK buffer was added to the cells, which were incubated and collected as described above, and combined together to form the Triton-soluble fraction which was then adjusted to 1% SDS. The remaining cellular material was extracted from the tissue culture dish with 1 ml of Western lysis buffer to generate the Triton-insoluble fraction. Both fractions were boiled with SDS-PAGE sample buffer for 5 min, and equivalent aliquots were analyzed by SDS-PAGE and immunoblotting.

Immunofluorescence cell staining. Cells were washed twice with Tris-Glu buffer, trypsinized, and counted by hemacytometer. Typically, 5×10^4 cells were plated on 22-by-22-mm glass coverslips (Fisher) placed in 35-mm dishes. Coverslips were routinely coated with poly-L-lysine (Sigma) for 30 min and allowed to dry prior to cell plating. At 40 h after being plated, cells were washed twice in 1× Hanks balanced salt solution (Gibco-BRL) and fixed at room temperature with 2% formaldehyde–0.05% glutaraldehyde–0.05% Triton X-100 for 20 min. After fixation, cells were washed twice with phosphate-buffered saline (PBS), incubated for 30 min in blocking solution (3% BSA and 0.05% Triton X-100 in PBS), and then incubated for 1 h with anti-paxillin, anti-vinculin, or anti-IGFR Ab. After three rinses with wash buffer (0.1% NP-40 in PBS), cells were incubated in the dark with FITC-conjugated anti-mouse or anti-rabbit secondary Abs or phalloidin for 1 h. Cells were rinsed three times with wash buffer and mounted onto microscope slides with the ProLong Antifade Kit (Molecular Probes) containing an antifade agent. Labeled cells were examined with an Olympus IX70 fluorescence microscope. Swiss 3T3 cells were fixed with 4% paraformaldehyde in PBS at room temperature for 20 min. After three washes with PBS, cells were permeabilized with 0.4% Triton X-100 for 3 min at room temperature. Anti-IGFR (1:200), anti-paxillin (1:50), anti-vinculin (1:50), anti-mouse IgG-FITC (1:200), and anti-rabbit IgG-FITC (1:200) Abs and phalloidin-FITC (1:200) and phalloidin-TRITC (1:200) were diluted in blocking buffer and centrifuged at maximum speed for 3 min prior to using the supernatant to label the cells.

TABLE 1. Interaction of RACK1 with IGF-IR in yeast is specific when compared to IR

Bait[a]	Prey[b]	Growth[c]	Color[d]
IGF-IR	Empty	No	−
IGF-IR	RACK1	Yes	++
IR	Empty	No	−
IR	RACK1	No	−
IR	Stat5bCT	Yes	++++

[a] The yeast two-hybrid interaction trap was used to examine the interaction of the tested proteins as described in Materials and Methods. Kinase active cytoplasmic domains of IGF-IR and IR were used as bait.
[b] Library plasmids isolated originally from two-hybrid screens were used as prey. pJG4-5 empty plasmid was used as control.
[c] Inducible colony growth after 48 h on galactose Leu$^-$ plates was compared to glucose Leu$^-$ plates.
[d] Inducible colony color on galactose–X-Gal (5-bromo-4-chloro-3-indolyl-β-D-galactopyranoside) plates was compared to that on glucose–X-Gal plates within 24 h. The number of "+" symbols indicates the relative intensity of the blue color, and the minus sign indicates white color.

Receptor internalization assay. Exponentially growing cells were trypsinized, counted, and seeded at a density of 10^6/10-cm dish. At 48 h after being plated, cells were incubated in serum-free DMEM for 20 h before incubation in serum-free DMEM supplemented with 100 ng of IGF-I/ml for 0, 2, 5, 10, 20, 30, or 50 min. Cells were placed on ice, washed twice with cold PBS containing 5 mM EDTA (PBS-EDTA), and collected by pipetting up and down in 4 ml of PBS-EDTA. Cells were incubated on ice with anti-IGFRα Ab diluted 1:100 in PBS-EDTA for 45 min. After 1 wash with cold PBS, cells were incubated on ice with anti-mouse IgG(H+L)-FITC secondary Ab diluted 1:50 in PBS for 30 min. After two washes with cold PBS, cells were fixed at room temperature with 8% formaldehyde in PBS for 30 min. After two washes with PBS, cells were resuspended in 1 ml of PBS and stored in the dark prior to flow cytometric analysis at the Mount Sinai cytometry facility.

Cell cycle analysis. Synchronization of cells in G_1 was accomplished by incubation of confluent cultures in DMEM with 0.5% BCS for 24 h. Cells were then incubated in DMEM with 2% BCS and 100 ng of IGF-I/ml for 48 h. Cells were washed twice in Tris-Glu buffer, trypsinized, and counted before and after treatment with IGF-I. Approximately 10^6 cells were removed and washed with cold PBS by gentle vortexing and centrifugation at 1,000 rpm (300 to 350 × *g*) for 5 min. Cells were then fixed at 4°C with 70% ethanol for 2 h. After two washes with PBS, cells were gently resuspended in 1 ml of DNA staining solution (PBS, pH 7.4; 1 μg of RNase A/ml; 20 μg of propidium iodide/ml). Samples were stored in the dark at 4°C prior to flow cytometry analysis at the Mount Sinai cytometry facility.

Monolayer cell growth. Exponentially growing cells were trypsinized, counted by hemacytometer, and plated at cell densities of 5×10^3 or 1×10^5 cells/35-mm dish as indicated in the figure legends. At 24 to 36 h after being plated, the cells were incubated in fresh growth medium containing 5 or 2% BCS, with or without IGF-I (100 ng/ml). Cells were counted on day 0 (i.e., the first day of medium change) and every other day thereafter. Medium with or without IGF-I was changed every other day.

Colony assay. Subconfluent cells in exponential growth were trypsinized, counted, and evenly resuspended at a density of 10^5 cells/3 ml of DMEM containing 0.3% Bacto Agar, antibiotics, and 7.5% BCS, with or without IGF-I (100 ng/ml). Cell suspensions were layered in 6-cm dishes over a 0.7% agar base containing the above components. Cells were grown at 37°C with addition of 0.5 ml of DMEM containing 7.5% BCS, plus 100 ng of IGF-I/ml where appropriate, every 3 to 4 days. After 4 weeks, colonies of >0.2 mm were counted from 10 randomly selected fields at ×40 magnification.

RESULTS

Isolation and initial characterization of RACK1, an IGF-I receptor-interacting protein. To identify proteins that could interact with the IGF-IR and possibly mediate its functions, we used the yeast two-hybrid interaction trap to screen a human (HeLa) cDNA library with the kinase-active cytoplasmic do-

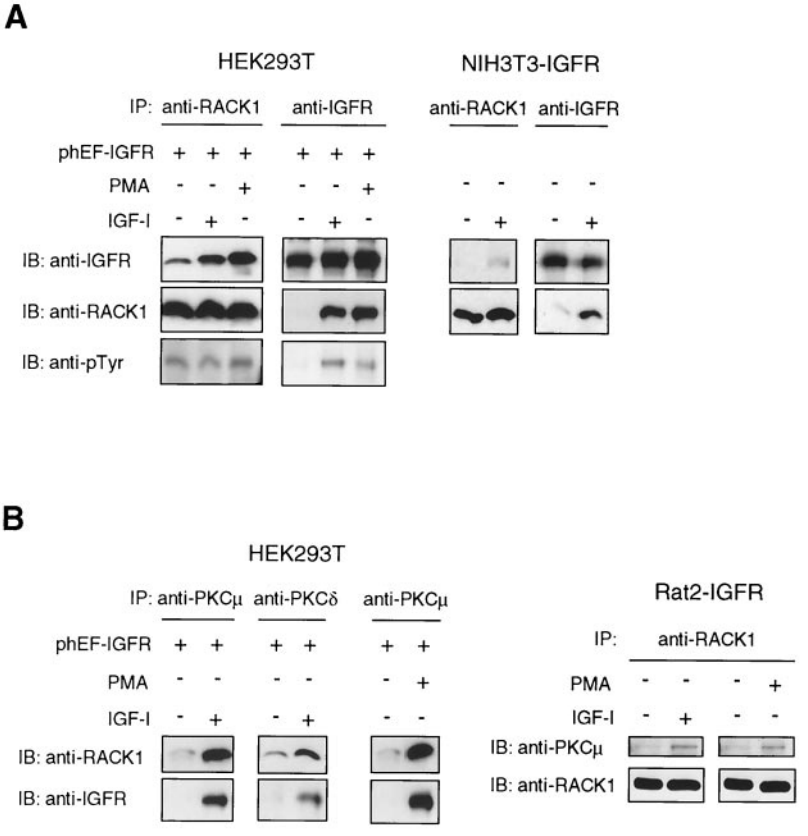

FIG. 1. IGF-I and PMA induce the intracellular association of RACK1, IGF-IR, and PKC. HEK293T cells transiently transfected with phEF-IGFR, NIH 3T3-IGFR cells, and Rat2-IGFR cells were serum starved overnight and either mock treated or treated with IGF-I or PMA for 10 min. Cell lysates were prepared with digitonin buffer. (A) A 1-mg portion of total cell lysate was immunoprecipitated (IP) with anti-RACK1 or anti-IGFR Ab (HEK293T and NIH 3T3-IGFR). Immunoprecipitates were fractionated by SDS–12% PAGE and transferred to a nitrocellulose membrane. The membrane was cut in half: the upper half was immunoblotted (IB) with anti-IGFR Ab (top panels), and the lower half was immunoblotted with anti-RACK1 Ab (middle panels). The membranes containing RACK1 (middle panel in the RACK1 IP) or IGF-IR (top panel in the IGFR IP) were stripped and reprobed with anti-phosphotyrosine Ab (anti-pTyr) (bottom panels). (B) A 1-mg portion of total cell lysate was immunoprecipitated with anti-PKCμ (HEK293T), anti-PKCδ (HEK293T), or anti-RACK1 (Rat2-IGFR) Ab. Immunoprecipitates were separated by SDS–12% PAGE and transferred to a membrane which was cut in half: the lower half was immunoblotted with anti-RACK1 (top panels of HEK293T), and the upper half was immunoblotted with anti-IGFR (bottom panels of HEK293T) or anti-PKCμ (top panels of Rat2-IGFR) Ab as shown.

main of IGF-IR as bait. Sequencing revealed that several of the cDNA clones isolated corresponded to the complete open reading frame of RACK1 (46). Repeated yeast two-hybrid analysis demonstrated that RACK1 interacted with IGF-IR but not with insulin receptor (IR) (Table 1). The carboxy tail of Stat5b (Stat5bCT), which we identified previously as an IR-interacting protein and showed to be a substrate of IR (16), was used as a positive control for interaction with IR. The interaction of RACK1 with IGF-IR but not with the closely related IR in yeast suggests that RACK1 could be involved in mediating functions specific to IGF-IR.

In vivo association of RACK1 with IGF-IR and PKC. To evaluate the interaction of RACK1 with IGF-IR in mammalian cells, HEK293T cells were transiently transfected with an IGF-IR expression plasmid, serum starved, and either mock treated or treated with IGF-I or PMA (Fig. 1A). Anti-RACK1 immunoprecipitates from digitonin-extracted cell lysates were fractionated by SDS-PAGE and immunoblotted with anti-IGFR to detect the association of IGF-IR with RACK1. Treatment of cells with IGF-I resulted in the enhanced coimmunoprecipitation of IGF-IR and RACK1 (Fig. 1A). An IGF-I-inducible association was similarly observed when cell lysates were reciprocally immunoprecipitated with anti-IGFR and immunoblotted with anti-RACK1 (Fig. 1A). Interestingly, association of RACK1 with IGF-IR was also induced when treated with PMA, a known activator of conventional and novel PKC isozymes, as demonstrated in HEK293T cells (Fig. 1A). In agreement with these results, similar treatment of NIH 3T3-IGFR cells, murine embryonic fibroblasts that stably overexpressed the human IGF-IR, also resulted in the IGF-I-dependent association of IGF-IR and RACK1 in reciprocal immunoprecipitation and immunoblotting experiments with anti-IGFR and anti-RACK1 (Fig. 1A). Similar results were obtained in Rat2-IGFR cells, rat fibroblasts that overexpressed the IGF-IR (data not shown). Similar experiments performed to detect the interaction between IR and RACK1 did not show any significant constitutive or insulin-inducible association of RACK1 with IR (data not shown), confirming the specificity of interaction observed in the yeast two-hybrid assay. Immunoblotting of anti-RACK1 immunoprecipitates with anti-pTyr

demonstrated that tyrosine phosphorylation of RACK1 was not significantly increased over the basal level of phosphorylation after treatment with either IGF-I or PMA (Fig. 1A), indicating that RACK1 is constitutively phosphorylated in these cells. Autophosphorylation of IGF-IR on tyrosine residues was significantly stimulated by IGF-I, as expected, but also by PMA, albeit to a lesser extent (Fig. 1A). These data indicate that, in mammalian cells, interaction of RACK1 with IGF-IR occurs in response to activation of IGF-IR by IGF-I and also in response to PMA stimulation, which implies that the interaction of RACK1 with IGF-IR may involve the activation of PKC. Our previous finding of activation of PKCδ by IGF-IR (32) is consistent with this notion.

RACK1 previously was shown to bind to activated PKC isozymes in vitro and has been demonstrated to be involved in PKCβII-mediated functions (48). Our results, demonstrating the PMA-inducible association of RACK1 with IGF-IR (Fig. 1A), prompted us to examine the intracellular interaction of PKC with RACK1 and with IGF-IR in mammalian cells. HEK293T cells were transiently transfected with IGF-IR, treated with IGF-I, and analyzed by immunoprecipitation with anti-PKC and immunoblotting with either anti-RACK1 or anti-IGF-IR (Fig. 1B). After treatment with IGF-I, PKCμ and PKCδ were associated with both RACK1 and IGF-IR. PMA treatment also led to an association of PKCμ with RACK1 and IGF-IR in these cells (Fig. 1B). In Rat2-IGFR fibroblasts, treatment with IGF-I and PMA each enhanced the association of RACK1 with PKCμ (Fig. 1B) but not with PKCα or PKCβ (data not shown). We suspect that the experimental conditions used were not sufficient to demonstrate the PMA-induced in vivo association of PKCβ and RACK1, which was reported previously (47). These results indicate that IGF-I and PMA are each capable of stimulating the association of certain PKC isozymes (δ and μ) with RACK1 and IGF-IR. Although these data together are not conclusive, they do suggest that activation of IGF-IR or PKC may lead to the formation of a protein complex comprised of IGF-IR, PKC, and RACK1 in mammalian fibroblast and epithelial cells.

Subcellular redistribution of RACK1 in oncogene-transformed mammalian and avian cells. We have previously characterized the activation of signaling pathways and biological behavior of mammalian and avian cells transformed by PTK oncogenes including those of the IR family. To begin to understand the potential role of RACK1 in cell transformation, we analyzed the subcellular distribution of RACK1 via P100 and S100 fractionation of oncogene-transformed cells and their respective untransformed controls. Subcellular fractionation of RACK1 in cell lines stably transformed by various oncogenes revealed a significant redistribution of RACK1 from the cytosolic to the membrane fraction in 3Y1 fibroblasts transformed by v-Src and RIE cells transformed by NM1 (encoding an oncogenic IGF-IR [35]) or T6 (encoding an oncogenic IR [43]) (Fig. 2A), but not in NIH 3T3 fibroblasts that were transformed by an activated H-Ras mutant (data not shown), compared to their respective controls. These results suggest that redistribution of RACK1 to the cellular membrane may be induced by PTK oncogenes. To further explore this idea, we infected CEF with NM1, UR2 (encoding the v-Ros PTK receptor-like oncogene [39]), or SR-A (encoding v-Src) virus and analyzed the subcellular distribution of RACK1 after the cells were morphologically transformed (Fig. 2B). Consistent with the results obtained in mammalian cells, there was a redistribution of RACK1 to the membrane fraction in NM1- and SR-A-infected cells compared to control CEF. Intriguingly, membrane localization of RACK1 was not observed in UR2-infected cells, suggesting that some but not all PTK receptor oncogenes can cause localization of RACK1 to the membrane (Fig. 2B). Furthermore, infection of CEF with the virus encoding *ts* kinase mutants of v-Src (*ts*Src), v-Ros (*ts*ROS), or NM1 (*ts*NM1) demonstrated that the oncogene-induced localization of RACK1 to the cellular membrane did not occur 2 h after the infected cells were shifted from a nonpermissive to a permissive temperature (Fig. 2C). At this time the PTKs of these oncogenes were found to be activated (data not shown). Translocation of RACK1 to the membrane occurred in CEF infected with *ts*Src and *ts*NM1 but not *ts*ROS after a 48-h shift to the permissive temperature (Fig. 2C) when full cellular morphologic transformation was clearly evident (data not shown), a finding which is in agreement with the results obtained with the constitutively activated versions of these oncogenes (Fig. 2B). Therefore, these results suggest that localization of RACK1 to the membrane does not occur as an immediate response to the kinase activity of these oncogenes. Instead, this redistribution may occur secondary to the transformation induced by certain oncogenic PTKs. However, the biological significance of the altered localization of RACK1 to the cellular membrane in such transformed cells is currently unclear.

Stable overexpression and subcellular distribution of RACK1 in NIH 3T3-IGFR cells. To examine the involvement of RACK1 in functions regulated by IGF-IR, we used PCR to generate full-length RACK1 with an HA epitope sequence at the carboxyl terminus (RACK1-HA) and cloned the PCR-generated products into an expression plasmid containing the promoter of the human elongation factor gene (phEF). Stable puromycin-resistant colonies were selected from NIH 3T3-IGFR cells that were cotransfected with the phEF-RACK1-HA expression plasmid and pBabePuro. The number of drug-resistant colonies in the RACK1-transfected cultures was comparable to that in the empty vector-transfected culture (data not shown), suggesting that expression of exogenous RACK1 was not overtly toxic to these cells. Expression levels of IGF-IR and RACK1 were determined by immunoblotting of total cell lysates with anti-IGFR and anti-RACK1 Abs, respectively (Fig. 3A). The presence of the HA epitope increases the apparent molecular weight of RACK1 more than expected, and the reason for the retarded mobility in SDS-PAGE is unclear. Clones expressing the highest levels of exogenous RACK1 (clones 1 and 4) had amounts comparable to levels of endogenous RACK1 and were used in most of the subsequent experiments. Coincidentally, these clones also expressed elevated levels of IGF-IR relative to control cells (Fig. 3A), which expressed levels similar to the parental NIH 3T3-IGFR cells (data not shown).

The intracellular localization of RACK1 in NIH 3T3-IGFR cells was determined by CSK subcellular fractionation. CSK fractionation revealed that the majority of RACK1 was associated with the Triton-insoluble fraction in control cells; a significant but much smaller amount of RACK1 was present in the Triton-soluble fraction (Fig. 3B). Surprisingly, a redistri-

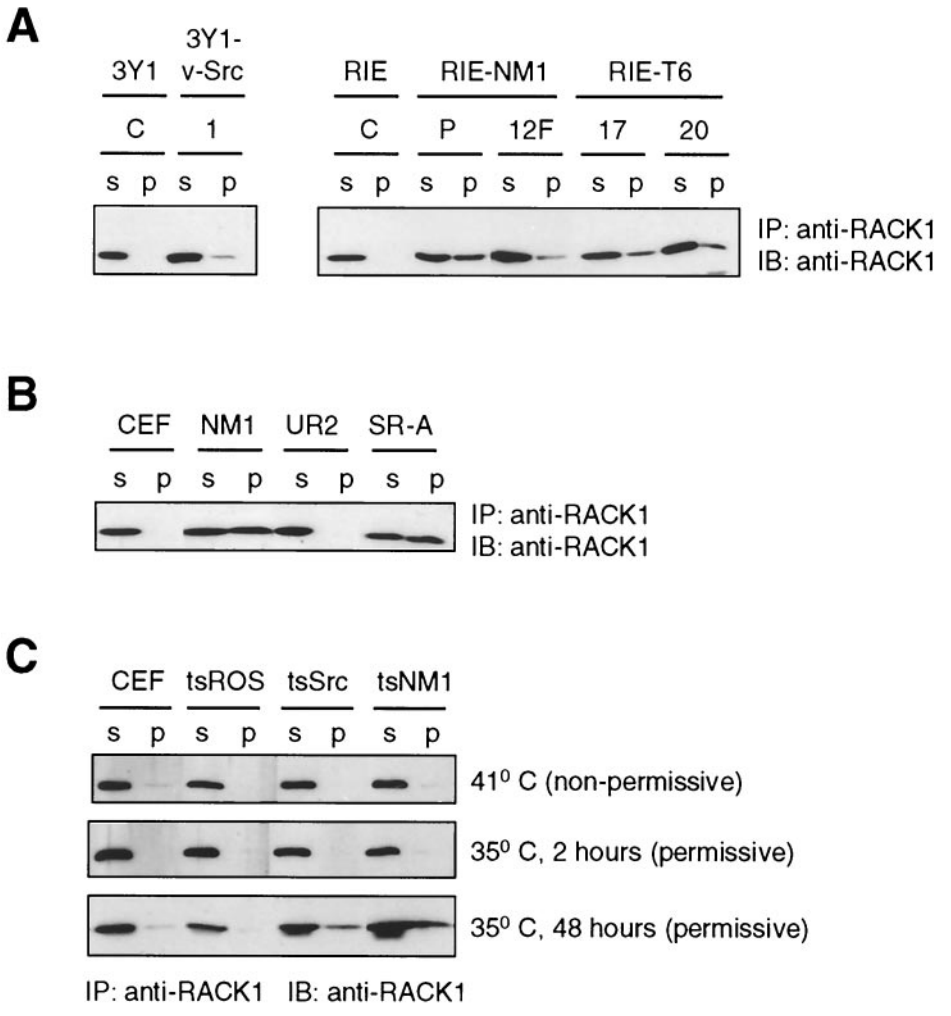

FIG. 2. RACK1 is redistributed to the membrane in oncogene-transformed avian and mammalian cells. Oncogene-transformed cells and their respective controls were fractionated into cytosolic S100 (S) and membrane P100 (P) fractions as described in Materials and Methods. Cell fractions were immunoprecipitated (IP) with anti-RACK1 Ab, resolved by SDS–10% PAGE, and transferred to a nitrocellulose membrane which was immunoblotted (IB) with anti-RACK1 Ab. (A) S100 and P100 fractions of 3Y1–v-Src (clone 2), RIE-NM1 (P, clone 12F), and RIE-T6 (clones 17 and 20) transformed cells were compared to their respective controls. (B) S100 and P100 fractions of CEF infected by NM1, UR2, and SR-A viruses were compared to uninfected CEF 3 days after infection. (C) CEF were infected with viruses encoding the *ts* mutants *ts*ROS, *ts*Src, and *ts*NM1. Infected and uninfected CEF were compared after 3 days at 41°C, after shifting them to 35°C for 2 h, or after shifting them to 35°C for 48 h. As a control experiment, cell lysates of *ts*NM1, *ts*Ros, and *ts*Src-infected CEF were immunoprecipitated with anti-IGFR, anti-Ros, and anti-Src Abs, respectively, separated by SDS–10% PAGE, and transferred to a nitrocellulose membrane which was sequentially immunoblotted with anti-phosphotyrosine Ab and the respective IP Ab. Our results demonstrated that the specific PTK activity of each *ts* mutant oncogene was increased substantially after 2 h at 35°C compared to 41°C (data not shown).

bution of both endogenous and exogenous RACK1 from the insoluble fraction to the soluble fraction was observed in stable RACK1-overexpressing cell lines (Fig. 3B). These results indicate that the majority of RACK1 is localized to a Triton-resistant cytoskeleton in NIH 3T3-IGFR cells and that overexpression of RACK1 in these cells shifts the localization of both endogenous and exogenous RACK1 away from the cytoskeleton toward other subcellular sites. Consistent with this notion, the association of RACK1 with IGF-IR, which was inducible by IGF-I in NIH 3T3-IGFR control cells (Fig. 3C) and in HEK293T cells that overexpressed IGF-IR but not RACK1 (Fig. 1A), was constitutive and no longer inducible by IGF-I in cells that stably overexpressed RACK1 (Fig. 3C). In P100–S100 fractionation experiments, we found no difference between control and RACK1-overexpressing cells in steady-state, unstimulated, or IGF-I-treated conditions in regard to the localization of RACK1, which was almost exclusively in the S100 cytosolic fraction and barely detectable in the P100 membrane fraction (data not shown), suggesting that overexpression of RACK1 does not involve a gross redistribution of RACK1 to the membrane but may involve only a subpopulation of RACK1 that associates with integral membrane proteins such as the IGF-IR (Fig. 3C).

RACK1 overexpression increases cell spreading, focal adhesions, and actin stress fibers. Initial observations that RACK1-overexpressing cells assumed a less-refractile appear-

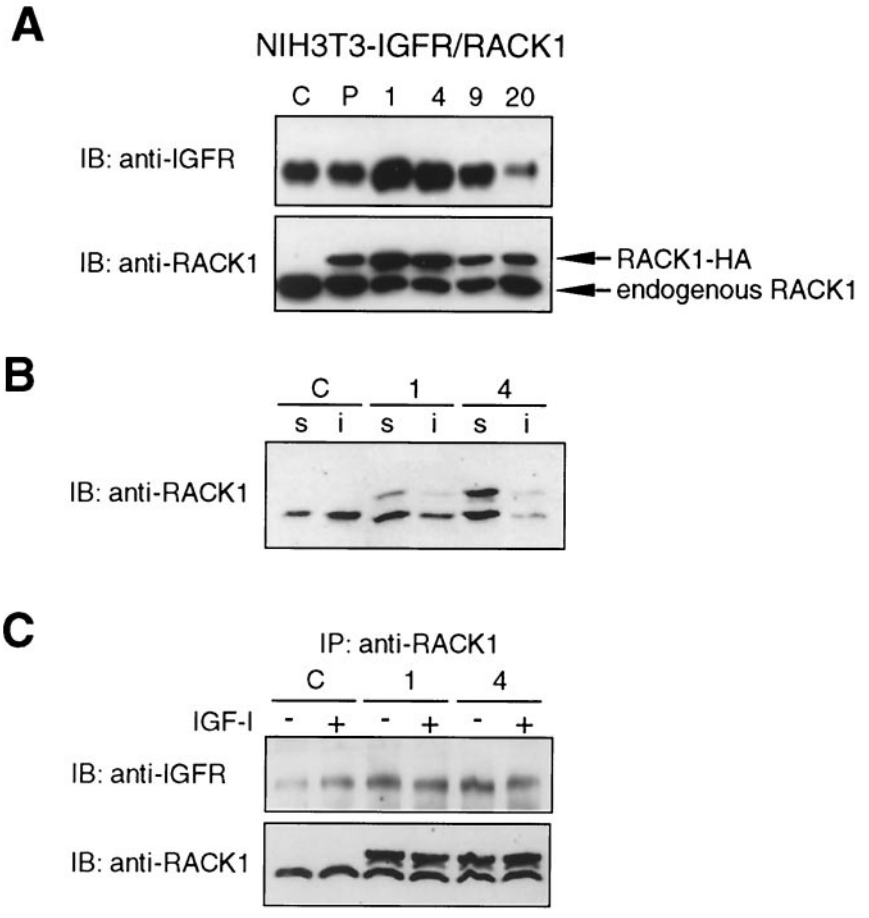

FIG. 3. Stable overexpression of RACK1 in fibroblasts results in its altered subcellular localization. (A) NIH 3T3-IGFR cells were cotransfected with pBabePuro and phEF-RACK1-HA or phEF-Neo and selected for puromycin resistance as described in Materials and Methods. RACK1-transfected clonal cell lines (clones 1, 4, 9, and 20), a culture composed of pooled RACK1-transfected clones (P), and the empty vector-transfected pooled culture (C) were established. Portions (10 μg) of RIPA-extracted total cell lysate protein from each cell line were fractionated by SDS–12% PAGE and transferred to a membrane which was cut in half and immunoblotted (IB) with anti-RACK1 (lower half) or anti-IGFR (upper half) Ab. Arrows indicate endogenous and exogenous (transfected) RACK1. (B) NIH 3T3-IGFR control (C) and RACK1-overexpressing cells (clones 1 and 4) were separated into Triton X-100-insoluble (i) and Triton X-100-soluble (s) fractions as described in Materials and Methods. Then, 10 μl of each fraction was separated in an SDS–12% polyacrylamide gel, transferred to a membrane, and immunoblotted with anti-RACK1 Ab. (C) Serum-starved control (C) and RACK1-overexpressing (clones 1 and 4) NIH 3T3-IGFR cells were mock treated or treated with IGF-I for 10 min. Cell lysates were prepared with 1% digitonin buffer and 1 mg of cell lysate was immunoprecipitated (IP) with anti-RACK1 Ab, resolved in an SDS–12% polyacrylamide gel, and transferred to a membrane which was cut in half and immunoblotted with anti-IGFR (upper half) or anti-RACK1 (lower half) Ab.

ance under light microscopy compared to control cells (Fig. 5A, right) suggested to us that RACK1 overexpression might alter the cytoskeleton and/or cellular adhesion properties of NIH 3T3-IGFR cells. To further investigate the effect of RACK1 overexpression on the actin cytoskeleton and focal adhesions, we used immunofluorescence microscopy to examine RACK1-overexpressing and control cells that were stained with phalloidin or Abs specific for paxillin and vinculin, proteins known to be present in focal adhesions (Fig. 4A). Phalloidin staining revealed that the total number of actin stress fibers in RACK1-overexpressing cells was generally increased with a distribution over a greater area per cell relative to control cells (Fig. 4A, top panels). Indeed, anti-IGFR staining showed that individual RACK1-overexpressing cells generally occupied a greater surface area (Fig. 4A, bottom panels), suggesting that overexpression of RACK1 results in increased spreading of NIH 3T3-IGFR cells. Anti-paxillin staining demonstrated that the total number of focal adhesions, particularly in areas away from the cell periphery, was increased in RACK1-overexpressing cells compared to control cells, in which focal adhesions were restricted primarily to the ends of cell projections, e.g., filopodia (Fig. 4A, second row). Staining with anti-vinculin Ab demonstrated a similar increase in focal adhesions in RACK1-overexpressing cells relative to control cells (Fig. 4A, third row). Together, these findings indicate that overexpression of RACK1 in NIH 3T3-IGFR cells results in an increase in cell spreading, which is consistent with an increase in focal adhesions and actin stress fibers within each cell.

We next examined the tyrosine phosphorylation of FAK and paxillin in exponentially growing cells under normal growth

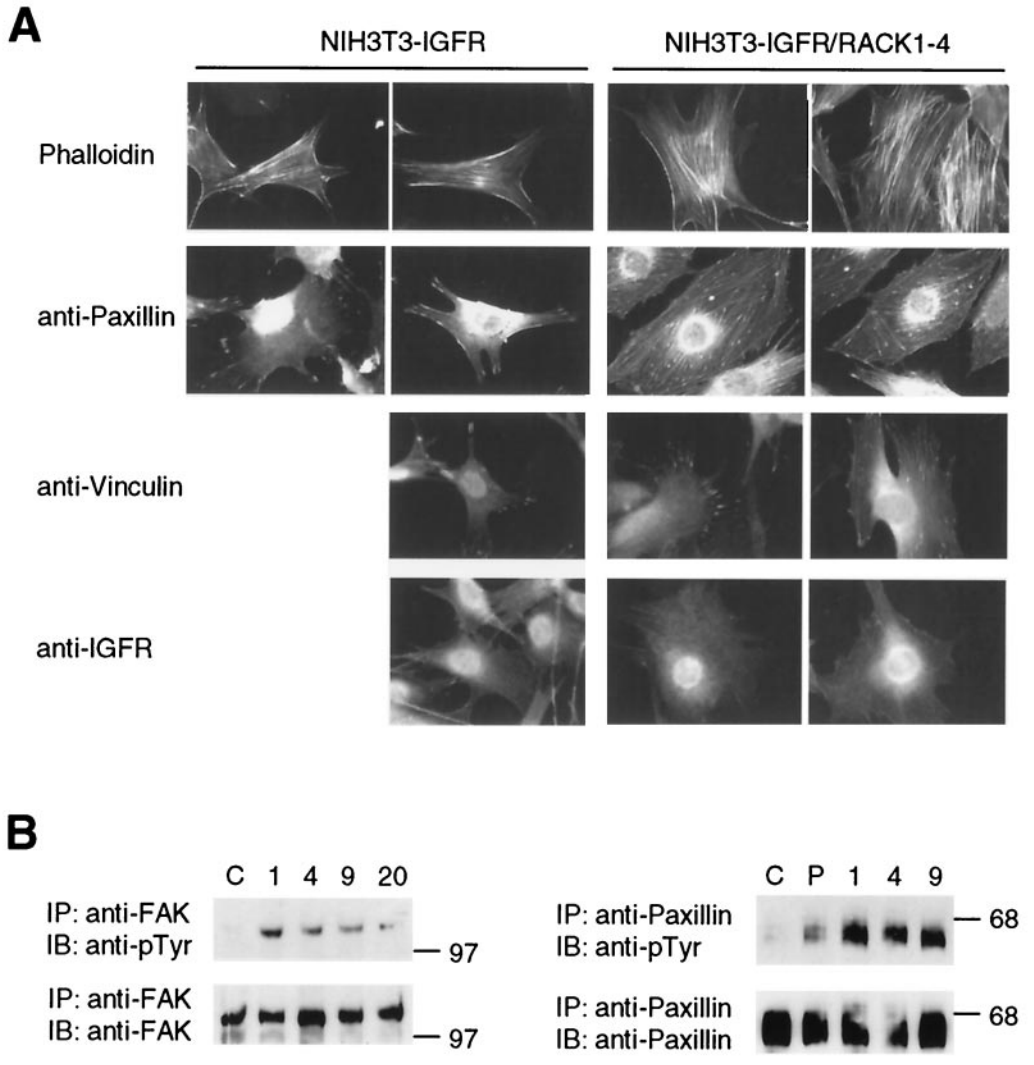

FIG. 4. Overexpression of RACK1 is correlated with increased cell spreading, actin stress fibers, focal adhesions, and tyrosine phosphorylation of FAK and paxillin. (A) Control and RACK1-overexpressing (clone 4) NIH 3T3-IGFR cells were fixed and stained with phalloidin-FITC (top row), anti-paxillin Ab (second row), anti-vinculin Ab (third row), or anti-IGFR Ab (bottom row) and examined by fluorescence microscopy. (B) Subconfluent cultures of control (C) and RACK-overexpressing (P; clones 1, 4, 9, and 20) cells were lysed with 0.5% NP-40 buffer. A total of 500 μg of total cell lysate was immunoprecipitated (IP) with anti-FAK or anti-paxillin Ab. Immunoprecipitates were separated in SDS–10% polyacrylamide gels and transferred to nitrocellulose membranes, which were immunoblotted (IB) with anti-phosphotyrosine Ab (anti-pTyr). The membranes were stripped and reprobed with anti-FAK or anti-paxillin Ab, as indicated.

conditions (Fig. 4B). Immunoprecipitation of cell lysates with anti-FAK (Fig. 4B, left) or anti-paxillin (Fig. 4B, right), followed by immunoblotting with anti-phosphotyrosine, revealed that steady-state tyrosine phosphorylation levels of FAK and paxillin were increased in RACK1-overexpressing NIH 3T3-IGFR cell lines relative to controls. These findings suggest that overexpression of RACK1 alters the phosphorylation of proteins of focal adhesion complexes. Moreover, these results are in agreement with previous studies that have correlated phosphorylation of FAK and paxillin with cell spreading (41, 44, 45), which is evident in cells that overexpress RACK1.

Overexpression of RACK1 inhibits IGF-I-dependent cell growth and transformation. Overexpression of RACK1 in NIH 3T3 cells was previously reported to inhibit the growth of those cells in normal growth conditions (13). We found that, consistent with this observation, RACK1 overexpression suppressed the exponential monolayer growth of NIH 3T3-IGFR cells (data not shown). Because RACK1 overexpression in NIH 3T3-IGFR cells caused an increase in cell spreading (Fig. 4A) and reduced light refractility of cells in confluent culture (Fig. 5A, right), we investigated whether RACK1 overexpression affected the ability of these cells to proliferate at high cell densities. Growth analysis of cells seeded initially at 75% confluence showed that both the initial growth rates and the final saturation densities of RACK1-overexpressing cell lines were 40 to 80% lower than those of the empty vector-transfected control cultures (Fig. 5A, left). These results were consistent among independent clones of RACK1-overexpressing cells

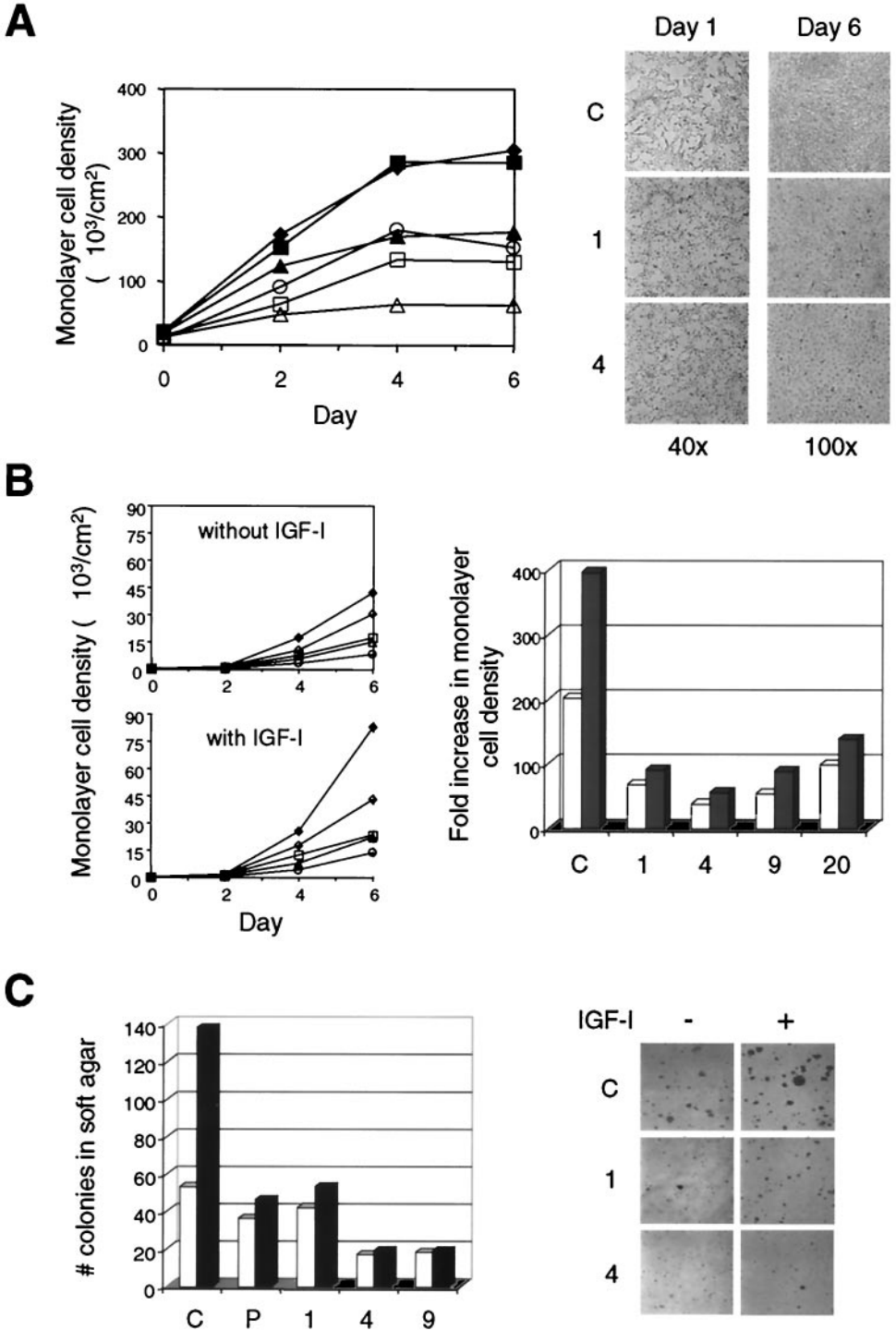

FIG. 5. RACK1 overexpression inhibits IGF-I-dependent monolayer cell proliferation and growth in soft agar. (A) Control (♦, clone 1; ■, clone 2) and RACK1-overexpressing (▲, P; ○, clone 1; ◇, clone 4; □, clone 20) NIH 3T3-IGFR cells were plated at a density of 10^5 cells/35-mm dish in medium containing 5% BCS and counted in duplicate every other day. Photomicrographs of control (C) and RACK1-overexpressing (clones 1 and 4) cells were taken on day 1 (at subconfluent cell density, ×40 magnification) and day 6 (at confluent cell density, ×100 magnification). (B) Control (♦, C) and RACK1-overexpressing (◇, clone 1; ○, clone 4; △, clone 9; □, clone 20) NIH 3T3-IGFR cells were plated at a density of 5×10^3 cells/35-mm dish in medium containing 2% BCS without (top graphs) or with (bottom graphs) supplemental IGF-I and counted in duplicate every other day. The histogram shows cell growth in the absence (open bars) or presence (shaded bars) of supplemental IGF-I as calculated by dividing the cell number on day 6 by the cell number on day 0. (C) Control (C) and RACK1-overexpressing (P; clones 1, 4, and 9) NIH 3T3-IGFR were seeded in soft agar without (open bar) or with (solid bar) supplemental IGF-I as described in Materials and Methods. Four weeks later, colonies (> 0.2 mm) were counted from 10 randomly selected low power (×40) microscopic fields. Photomicrographs show representative colony sizes at ×40 magnification.

and suggest that overexpression of RACK1 suppresses cell growth in monolayer cultures at both low and high cell densities.

The association of RACK1 with IGF-IR after its activation by IGF-I (Fig. 1A) suggests that RACK1 plays a direct role in the biological functions mediated by IGF-IR. We chose to examine the effect of RACK1 overexpression in NIH 3T3 cells that stably expressed human IGF-IR at levels two- to threefold above the endogenous IGF-IR level because it would allow us to analyze IGF-I-inducible cell proliferation in both anchorage-dependent (i.e., monolayer) and anchorage-independent (i.e., soft agar) conditions since NIH 3T3 cells expressing elevated levels of IGF-IR can be induced by IGF-I to form colonies (29, 32, 35). To determine the effect of RACK1 overexpression on IGF-I-dependent monolayer growth, equivalent numbers of RACK1-overexpressing and control cells were seeded in medium containing a low concentration of serum with or without supplemental IGF-I, and cell numbers were subsequently determined at regular intervals (Fig. 5B). In the presence of only a low concentration of serum, the growth rate of each RACK1-overexpressing cell line was inhibited relative to control NIH 3T3-IGFR cells at all of the time points examined. The addition of exogenous IGF-I significantly stimulated the growth rate of the control cells but not of the RACK1-overexpressing cells. A comparison of the IGF-I-dependent increase in cell density after 6 days showed that the growth of NIH 3T3-IGFR control cells was stimulated by 100% compared to 30 to 60% for the RACK1-overexpressing cells. These results indicate that overexpression of RACK1 inhibits IGF-I-inducible cell growth in anchorage-dependent conditions.

To determine the effect of RACK1 overexpression on IGF-I-induced anchorage-independent growth, we analyzed the colony-forming ability in soft agar of control and RACK1-overexpressing NIH 3T3-IGFR cells. As expected, the number of colonies in control cultures that were supplemented with IGF-I was increased by 160% (Fig. 5C). In contrast, the colony growth of RACK1-overexpressing cells was increased by only 6 to 28% (Fig. 5C), indicating that overexpression of RACK1 significantly suppresses the IGF-I-mediated anchorage-independent growth of NIH 3T3-IGFR cells. Independent stable clones that overexpressed RACK1 with either an amino-terminal HA epitope (HA-RACK1) or a carboxyl-terminal histidine tag (RACK1-His) also displayed a reduction of IGF-I-induced colony formation (data not shown), providing additional evidence for a role of RACK1 in cell transformation. Together, these data demonstrate that overexpression of RACK1 inhibits IGF-I-dependent growth under both anchorage-independent and anchorage-dependent conditions, thus implicating RACK1 in IGF-IR-mediated biological functions.

Activation of IGF-IR and its major signaling pathways are not affected. To explore potential mechanisms that may account for the alteration of IGF-I-dependent cell proliferation and transformation in NIH 3T3-IGFR cells, we next examined the major IGF-IR-mediated signal transduction pathways. Control and RACK1-overexpressing cells were serum starved, treated with IGF-I for up to 50 min, and analyzed for the activation and internalization of IGF-IR, the tyrosine phosphorylation and activation of the major IGF-IR substrates Shc and IRS-1, and the activation of components of the PI3K and MAPK pathways (Fig. 6). Overall, our results indicate that there were no significant differences between RACK1-overexpressing and control cells in the early activation kinetics of any of the signaling molecules examined. The IGF-I-stimulated internalization of IGF-IR was detectable as early as 2 min and peaked after 20 min of IGF-I treatment (Fig. 6A). Tyrosine phosphorylation of IGF-IR reached a maximum within 2 min of IGF-I treatment and decreased dramatically after 10 min (Fig. 6B), indicating that overexpression of RACK1 does not affect receptor autophosphorylation, activation, and internalization induced by IGF-I. Tyrosine phosphorylation of IRS-1, association of IRS-1 with $p85^{PI3K}$ and PI3K activity, and phosphorylation of Akt/PKB, a downstream effector of PI3K which is activated by the lipid products of PI3K, were detectable within 2 min, persisting above unstimulated level for at least 50 min (Fig. 6B). The activating phosphorylation of $p70^{S6K}$, another downstream effector of PI3K, was detectable after 20 min and persisted for at least 50 min (Fig. 6B). The overall increased association of IRS-1 with $p85^{PI3K}$ and PI3K activity is consistent with the slightly elevated IRS-1 level in this RACK1-overexpressing cell line (data not shown). The IGF-I-stimulated tyrosine phosphorylation of Shc was detectable within 2 min and returned to basal levels within 50 min (Fig. 6B). The phosphorylation of ERK1 and ERK2 on activating tyrosine and threonine residues was markedly increased at 2 min, reached a maximum at 5 min, and remained above basal levels after 50 min of IGF-I treatment (Fig. 6B). Together, these data suggest that overexpression of RACK1 does not affect the IGF-I-dependent activation and internalization of IGF-IR and the IGF-I-mediated activation of downstream signal transduction pathways involving Shc, IRS-1, PI3K, and MAPK.

RACK1 overexpression perturbs IGF-I-dependent integrin-mediated signaling. Because RACK1 has been shown to associate with β1 integrin in response to PMA (33), we investigated the involvement of IGF-IR in the association of RACK1 with β1 integrin. HEK293T cells were transiently transfected with an IGF-IR expression plasmid, serum starved, and either mock treated or treated with IGF-I or PMA. Anti-β1 integrin immunoprecipitates from digitonin-permeabilized cell extracts were immunoblotted with anti-RACK1 or anti-IGFR, demonstrating that both RACK1 and IGF-IR associated with β1 integrin in response to treatment with either IGF-I or PMA (Fig. 7A). This finding suggests that, upon activation of IGF-IR or PKC, RACK1 forms a protein complex that includes IGF-IR and β1 integrin, providing a potential mechanism by which these molecules could regulate one another. Previous studies have provided evidence for the involvement of RACK1 in the regulation of c-Src and PKC (13, 47), mediators of integrin signaling, which prompted us to explore the role of RACK1 in the regulation of IGF-I-dependent protein kinase activity within integrin-associated complexes. We examined β1 integrin-associated kinase activity by performing in vitro kinase assays on anti-β1 integrin immunoprecipitates in NIH 3T3-IGFR and HEK293T cells (Fig. 7B and C, respectively). In control NIH 3T3-IGFR cells (Fig. 7B) and HEK293T cells transiently transfected with IGF-IR and empty vector plasmids (Fig. 7C), treatment with IGF-I led to a significant increase in the protein kinase activity associated with β1 integrin, as reflected by the enhanced in vitro phosphorylation of protiens of 120 and 80 kDa in NIH 3T3-IGFR cells and of proteins of 140

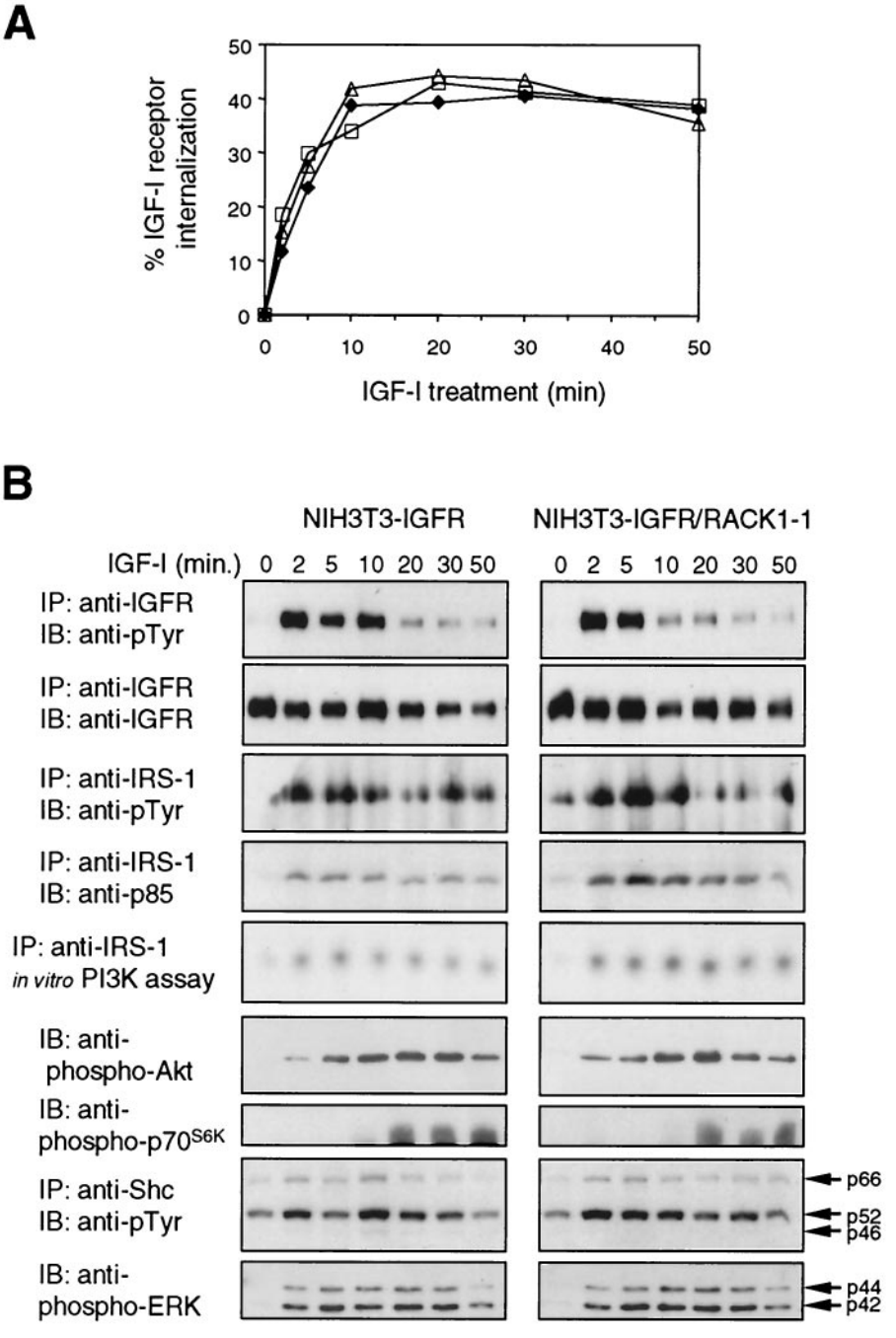

FIG. 6. IGF-I-mediated internalization and autophosphorylation of IGF-IR- and IGF-I-dependent MAPK and PI3K signaling are unaffected by RACK1 overexpression. (A) Control (♦, clone 1) and RACK1-overexpressing (△, clone 1; □, clone 4) NIH 3T3-IGFR cells were seeded at a density of 10^6/10-cm dish. At 48 h after being plated, the cells were serum starved for 20 h prior to treatment with IGF-I for 0, 2, 5, 10, 20, 30, or 50 min. Internalization of IGF-IR was analyzed by flow cytometry as described in Materials and Methods. (B) Control and RACK1-overexpressing NIH 3T3-IGFR cells were grown to confluence, serum starved, and treated 24 h later with IGF-I for 0, 2, 5, 10, 20, 30, or 50 min. Cell lysates were prepared with 1% NP-40 buffer, and 500 μg of total cell lysate was immunoprecipitated (IP) with anti-IGFR, anti-IRS-1, or anti-Shc Ab as indicated. Immunoprecipitates were run in SDS–10% polyacrylamide gels, transferred to nitrocellulose membranes, and immunoblotted (IB) with anti-phosphotyrosine Ab (anti-pTyr). Membranes were stripped and reprobed with anti-IGFR or anti-p85 (PI3K) Ab as indicated. Parallel anti-IRS-1 immunoprecipitates were analyzed for in vitro PI3K activity as described in Materials and Methods. A total of 10 μg of each cell lysate was resolved by SDS–10% PAGE and immunoblotted with anti-phospho-Akt, anti-phospho-$p70^{S6K}$, or anti-phospho-ERK Ab. Arrows indicate p46, p52, and p66 Shc isoforms and p42 and p44 MAPKs.

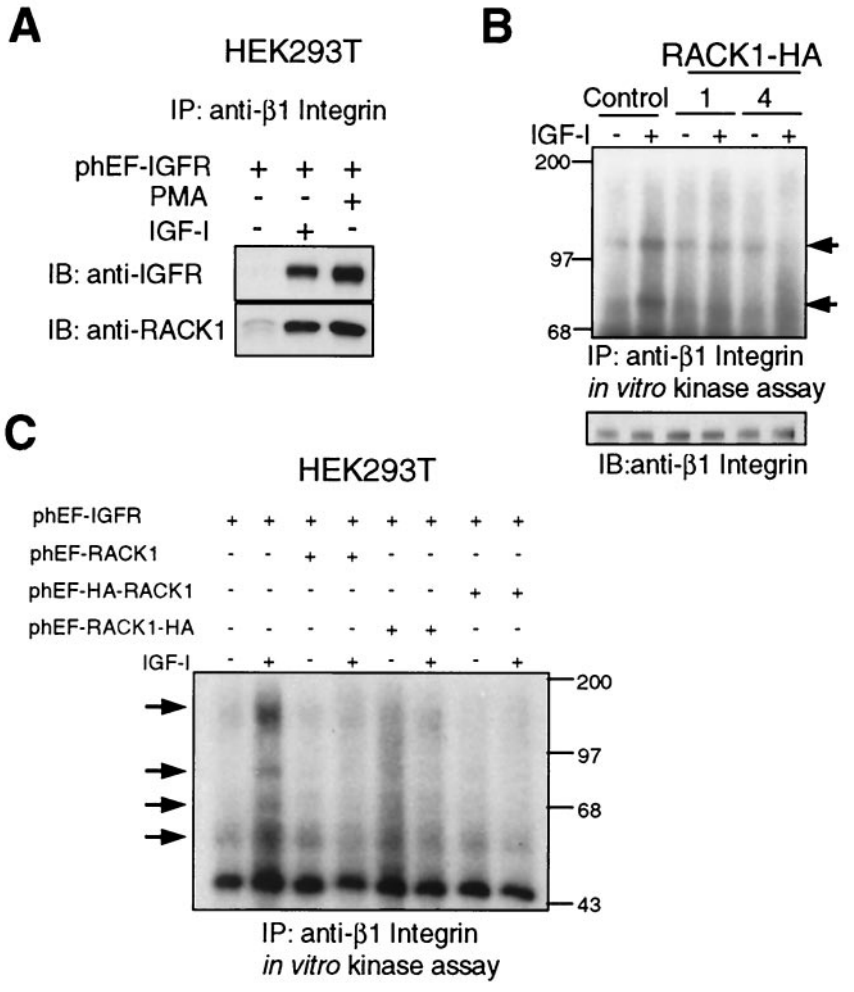

FIG. 7. IGF-I and PMA induce the association of IGF-IR, RACK1, and β1 integrin, and RACK1 overexpression inhibits IGF-I-dependent β1 integrin-associated kinase activity. (A) HEK293T cells were transiently transfected with phEF-IGFR, serum starved, and either mock treated or treated with IGF-I or PMA for 10 min as described in Materials and Methods. Cell lysates were prepared with digitonin buffer, and 1 mg of total lysate was immunoprecipitated (IP) with anti-β1 integrin Ab. Immunoprecipitates were fractionated in an SDS–12% polyacrylamide gel and transferred to a nitrocellulose membrane, which was cut in half and immunoblotted (IB) with anti-IGFR (upper half) or anti-RACK1 (lower half) Ab. (B) Control and RACK1-overexpressing (clone 1 and 4) NIH 3T3-IGFR cells were serum starved overnight and treated with IGF-I for 10 min. Cell lysates were prepared with CHAPS buffer, and 500 μg of total lysate was immunoprecipitated with anti-β1 integrin Ab and analyzed for in vitro kinase activity as described in Materials and Methods. Arrows indicate the proteins phosphorylated in vitro (upper panel). Equivalent amounts of lysates were analyzed directly by fractionation in SDS–10% polyacrylamide gels and immunoblotting with anti-β1 integrin Ab (lower panel). (C) HEK293T cells were transiently cotransfected with the indicated plasmids as detailed in Materials and Methods, serum starved, and treated with IGF-I as described for panel B. Arrows indicate the proteins phosphorylated in vitro.

to 150, 80, 65, and 55 to 60 kDa in 293T cells that coimmunoprecipitated with β1 integrin (Fig. 7B and C, respectively). In contrast, the IGF-I-dependent phosphorylation of these proteins was dramatically reduced in RACK1-overexpressing NIH 3T3-IGFR cells (clones 1 and 4) and in HEK293T cells that were cotransfected with IGF-IR and either RACK1, RACK1-HA, or HA-RACK1 plasmids (Fig. 7B and C, respectively). These results suggest that IGF-IR may modulate the protein kinase activity of β1 integrin complexes in a manner which is dependent on IGF-I and RACK1. Suppression of IGF-I-inducible integrin-associated kinase activity by RACK1 overexpression may lead to the disruption of integrin signaling and integrin functions.

Previous reports have suggested that IGF-IR may play a role in regulating the functions of molecules associated with focal adhesions. The IGF-I-dependent tyrosine phosphorylation of focal adhesion molecules FAK, paxillin, and $p130^{CAS}$, as well as the IGF-I-mediated association of $p130^{CAS}$ and Crk, have been described (3, 12). Our data in Fig. 7 prompted us to investigate the role of RACK1 in the IGF-I-dependent tyrosine phosphorylation and association of focal adhesion proteins that are thought to be involved in integrin signaling. We examined the effect of RACK1 overexpression on the response of focal adhesion proteins after IGF-I treatment in NIH 3T3-IGFR cells. IGF-I treatment of control cells mildly and transiently increased the tyrosine phosphorylation of $p130^{CAS}$ over the basal level, reaching a maximum within 2 min and returning to the basal level by 10 min (Fig. 8A). In contrast, the

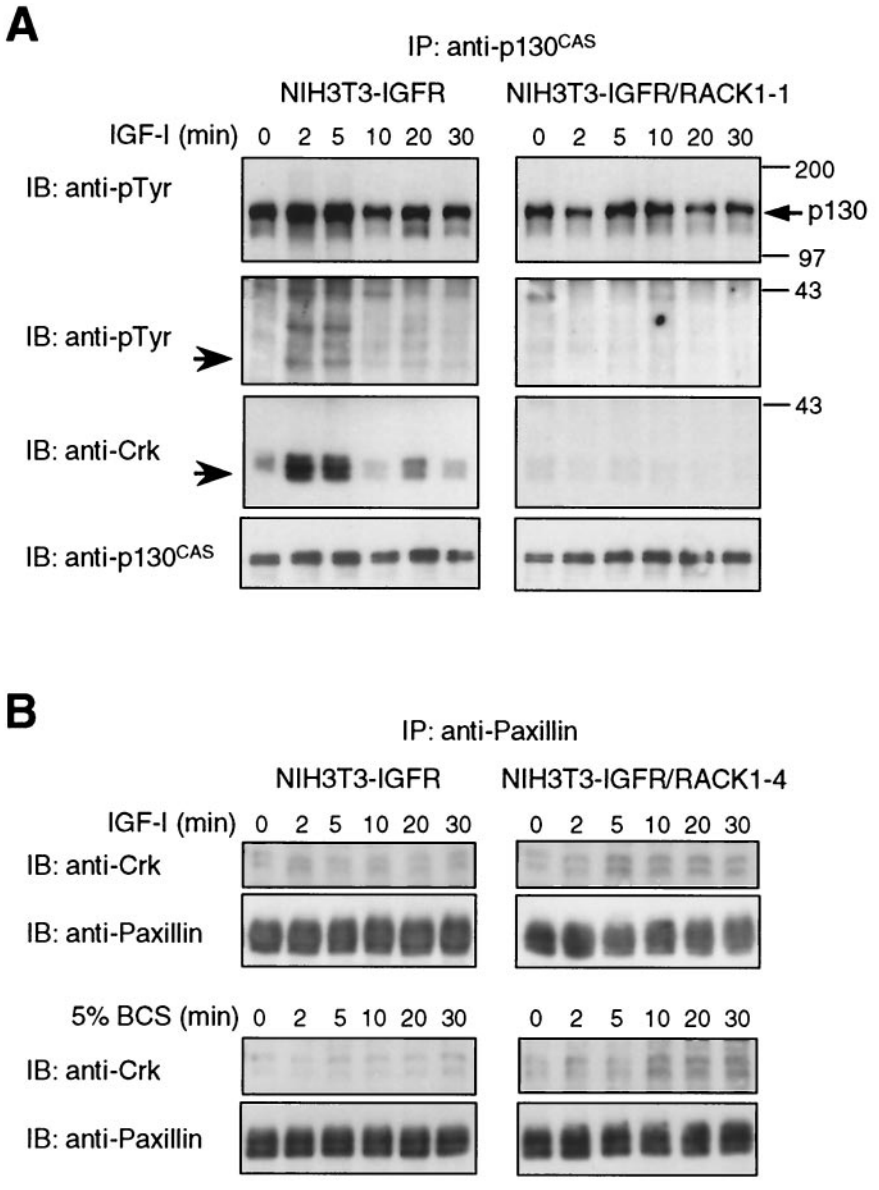

FIG. 8. Overexpression of RACK1 disrupts IGF-I-dependent signaling mediated by focal adhesion proteins. (A) Control and RACK1-overexpressing (clone 1) NIH 3T3-IGFR cells were grown to confluence and then serum starved; 24 h later they were treated with IGF-I for 0, 2, 5, 10, 20, or 30 min. Cell lysates were prepared with 1% NP-40 buffer, and 500 μg of total lysate was immunoprecipitated (IP) with anti-p130^{CAS} Ab. Immunoprecipitates were separated in SDS–12% polyacrylamide gels, transferred to nitrocellulose membranes, and immunoblotted (IB) with anti-phosphotyrosine Ab (top two rows). Membranes were stripped, cut in half, and reprobed with anti-Crk (third row) or anti-p130^{CAS} (bottom row) Ab. The large arrowheads indicate the corresponding positions of Crk. (B) Control and RACK1-overexpressing (clone 4) NIH 3T3-IGFR cells were grown to confluent cell density and then serum starved; 24 h later they were treated with IGF-I (upper two rows) or BCS (lower two rows) for 0, 2, 5, 10, 20, or 30 min. Cell lysates were prepared with 1% NP-40 buffer, and 500 μg of total lysate was immunoprecipitated with anti-paxillin Ab. Immunoprecipitates were separated in SDS–10% polyacrylamide gels, transferred to nitrocellulose membranes, and immunoblotted with anti-Crk Ab. Membranes were stripped and reprobed with anti-paxillin Ab.

IGF-I-dependent tyrosine phosphorylation of p130^{CAS} was reduced and delayed in cells that overexpressed RACK1, appearing after 5 min of IGF-I treatment (Fig. 8A). Futhermore, IGF-I treatment led to the association of p130^{CAS} with a number of tyrosine-phosphorylated proteins, including a 36-kDa protein (Fig. 8A, second row, indicated by the arrow), observed in control cells but not in RACK1-overexpressing cells. Stripping the membranes and reprobing with anti-Crk revealed that the 36-kDa protein corresponded to Crk (Fig. 8A, third row). Therefore, the IGF-I-inducible association of p130^{CAS} with Crk was suppressed in the RACK1-overexpressing cells. The levels of p130^{CAS} remained unchanged with IGF-I treatment in both control and RACK1-overexpressing cells (Fig. 8A, bottom row). The mildly delayed and reduced tyrosine phosphor-

ylation of $p130^{CAS}$, as well as the suppression of $p130^{CAS}$-Crk association, was similarly observed in another RACK1-overexpressing cell line (clone 4) (data not shown). These data indicate that overexpression of RACK1 attenuates the IGF-I-induced tyrosine phosphorylation of $p130^{CAS}$ and disrupts the formation of a $p130^{CAS}$-Crk complex. These results are also consistent with the suppression of IGF-I-stimulated β1 integrin-associated kinase activity observed in cells overexpressing RACK1 (Fig. 7B).

Paxillin, another component of the focal adhesion complex (5), was shown to associate with v-Crk, and therefore we investigated the possible association of endogenous c-Crk with paxillin and the effect of RACK1 overexpression on this process. Immunoblotting of anti-paxillin immunoprecipitates with anti-Crk revealed that the association of Crk and paxillin in RACK1-overexpressing cells was noticeably increased in response to treatment with IGF-I or serum compared to control cells (Fig. 8B). While the association of paxillin and Crk after IGF-I treatment was marginal in control cells, a significant association between paxillin and Crk was observed after 5 min of IGF-I treatment of RACK1-overexpressing cells (Fig. 8B, upper panels). Consistent with this result, treatment with serum also stimulated a significant but slightly delayed paxillin-Crk interaction in RACK1-overexpressing cells (Fig. 8B, lower panels). The lower concentration of IGF-I in 5% serum may account for the delayed response. This result, which was also observed in another RACK1-overexpressing cell line (clone 1) (data not shown), suggests that overexpression of RACK1 potentiates the formation of an IGF-I-inducible paxillin-Crk complex. Therefore, overexpression of RACK1 appears to alter the association between Crk and proteins of the focal adhesion complex and is likely to result in altered integrin-mediated downstream signaling.

RACK1 overexpression inhibits cell cycle progression by altering cell cycle regulators. To further explore the mechanism by which overexpression of RACK1 inhibits cell proliferation, we analyzed cell cycle progression in control and RACK1-overexpressing cells by measuring cellular DNA content by flow cytometry analysis after the synchronization of confluent cultures in G_0 by serum withdrawal and the subsequent release into G_1 and S by treatment with IGF-I (Fig. 9A). We determined the minimum concentration of serum necessary for IGF-I-dependent cell cycle progression in control NIH 3T3-IGFR cells to be 2% BCS (data not shown). After treatment with IGF-I and BCS for 48 h, a significant proportion of control cells (at least 30%) had entered S phase compared with cells that overexpressed RACK1, which were predominantly (>95%) in G_0 or G_1 (Fig. 9A). This suggests that overexpression of RACK1 in NIH 3T3-IGFR cells leads to inhibition of cell cycle progression in G_0, in G_1, or at the G_1/S transition point and is consistent with the delay in G_1 progression observed in an unsynchronized population of NIH 3T3 cells that overexpressed RACK1 (13). Interference of IGF-I-induced cell cycle progression in NIH 3T3-IGFR cells is likely to underlie the suppression of IGF-I-mediated anchorage-independent and anchorage-dependent growth observed in these cells.

To identify alterations in the regulation of the G_1 and S phases of the cell cycle, we examined the phosphorylation state of Rb and the expression levels of cyclins, Cdks, and CKIs that are known to regulate the G_1 and S phases of the cell cycle. In exponentially growing control cells, the majority of the Rb protein was hyperphosphorylated in comparison with RACK1-overexpressing cell lines, in which Rb protein was present mainly in the hypophosphorylated state (Fig. 9B). The expression levels of cyclin D1, cyclin E, cyclin A, Cdk4, Cdk6, and Cdk2 were comparable among RACK1-overexpressing and control cells (Fig. 9C). Interestingly, the levels of the $p21^{Cip1/WAF1}$ and $p27^{Kip1}$ CKIs in cells that overexpressed RACK1 were significantly increased above those in control cells (Fig. 9C). These findings indicate that overexpression of RACK1 leads to the hypophosphorylation of Rb protein, a regulator of the G_1/S transition. Furthermore, the data suggest that the mechanism may involve the accumulation of $p21^{Cip1/WAF1}$ and $p27^{Kip1}$, CKIs that are known to inhibit the kinase activity of cyclin-Cdk2 complexes, which are able to phosphorylate target proteins such as Rb. These results together are consistent with the delay in cell cycle progression in RACK1-overexpressing cells (Fig. 9A).

The effect of RACK1 overexpression on the regulation of IGF-I-dependent cell cycle regulation was further examined in these cells. IGF-I treatment of cells for 12 h led to a significant reduction in the level of $p27^{Kip1}$ concomitant with a dramatic increase in cyclin E-associated kinase activity in control cells (Fig. 9D). However, the extent of these changes in $p27^{Kip1}$ and cyclin E-associated kinase activity was significantly attenuated in RACK1-overexpressing cells (Fig. 9D). Not surprisingly, the $p27^{Kip1}$ level in control cells was increased to a level similar to that of RACK1-overexpressing cells upon serum starvation (Fig. 9D). Collectively, these data indicate that overexpression of RACK1 leads to the upregulation of CKIs with a corresponding suppression of Cdk2 activity and Rb phosphorylation, which may at least partially account for the inhibition of IGF-I-stimulated monolayer and anchorage-independent growth observed in these cells.

Blockade of endogenous RACK1 expression by antisense oligonucleotides inhibits cell spreading and cell proliferation. To more precisely establish the function of endogenous RACK1 and to confirm our results from an overexpression system, which may produce nonphysiologic effects, we used antisense oligonucleotides designed to block RACK1 translation, in an attempt to suppress the level of endogenous RACK1 protein and to examine the effect on cell morphology and monolayer proliferation. After unsuccessful attempts with phosphorothioate oligonucleotides and antisense expression vectors, we chose to use morpholino oligonucleotides, which are extremely stable and have recently been used successfully to block the expression and function of endogenous proteins (56). Standard control or RACK1 antisense morpholino oligonucleotides were introduced into Swiss 3T3 cells according to the method recommended by the manufacturer as described in Materials and Methods. An effect on cell morphology and cell proliferation was not immediate and only became evident at least 4 days after introduction of oligonucleotides, which may be explained by the high stability of RACK1 protein ($t_{1/2}$ = 40 h [data not shown]) and/or suboptimal intracellular concentrations of antisense morpholino oligonucleotide. Beginning 4 days after the introduction of oligonucleotides, Swiss 3T3 cells with antisense oligonucleotides were observed to adopt a more refractile appearance under light microscopy compared to control cells (Fig. 10A, upper left panels) and parental cells (data

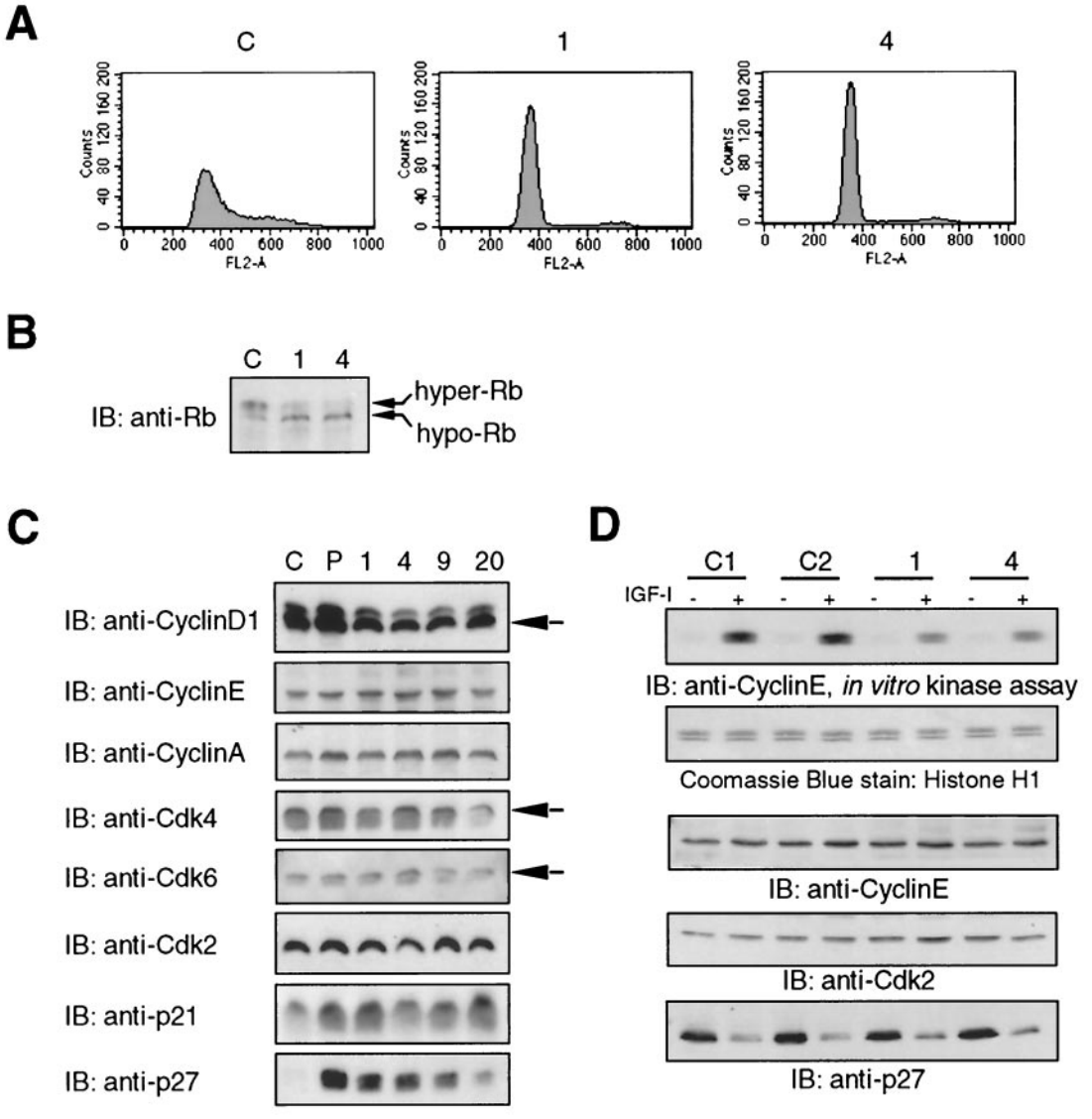

FIG. 9. RACK1 overexpression leads to Rb hypophosphorylation, increased levels of CKIs, and inhibition of IGF-I-dependent G_1 cell cycle progression and cyclin E-associated Cdk activity. (A) Control and RACK1-overexpressing (clones 1 and 4) NIH 3T3-IGFR cells were synchronized and held in G_0/G_1 by incubation in growth factor-depleted growth medium (0.5% BCS) for 24 h and then released by incubation in growth medium containing 2% BCS with IGF-I for 48 h. The cell cycle distribution was analyzed by flow cytometry as described in Materials and Methods. The histograms represent the cell cycle distribution after 48 h of IGF-I stimulation. (B) Control (C) and RACK1-overexpressing (clones 1 and 4) NIH 3T3-IGFR cells were lysed with Western extraction buffer. Then, 50 μg of total cell lysate was fractionated in an SDS–7.5% polyacrylamide gel, transferred to nitrocellulose, and immunoblotted (IB) with anti-Rb Ab. Arrows indicate the hyper- and hypophosphorylated forms of Rb. (C) Cell lysates of control (C) and RACK1-overexpressing (P; clones 1, 4, 9, and 20) NIH 3T3-IGFR cells were prepared with Western extraction buffer. A total of 10 μg of total cell lysate was separated in parallel SDS–12% polyacrylamide gels, transferred to nitrocellulose, and immunoblotted with anti-cyclin D1, anti-cyclin E, anti-cyclin A, anti-Cdk4, anti-Cdk6, anti-Cdk2, anti-p21, or anti-p27 Ab as indicated. (D) Two independent control (C1 and C2) and RACK1-overexpressing (clones 1 and 4) NIH 3T3-IGF-IR cell lines were serum starved for 24 h and then either treated with IGF-I for 12 h or left untreated. A total of 200 μg of protein lysate was immunoprecipitated with anti-cyclin E Ab and subjected to in vitro kinase assay by using histone H1 as the substrate (top panel) as described in Materials and Methods. Coomassie blue staining shows the amount of histone H1 protein loaded in each lane (second panel). Then, 20 μg of total cell extract was separated in parallel SDS–12% polyacrylamide gels, transferred to nitrocellulose, and immunoblotted with anti-cyclinE, anti-Cdk2, or anti-p27 Ab to assess the levels of cyclin E, Cdk2, and $p27^{Kip1}$.

not shown). Analysis of cell morphology by fluorescence staining with phalloidin demonstrated that, while control cells assumed a spread phenotype similar to that of parental cells, antisense oligonucleotide-treated cells generally displayed a more contracted and less spread morphology (Fig. 10A). Costaining with phalloidin and antivinculin to assess the actin cytoskeleton and focal adhesions, respectively, demonstrated fewer stress fibers in antisense oligonucleotide-treated cells compared to control cells, which were also found to possess a greater number of focal adhesions that were distributed throughout the cell (Fig. 10B). After introduction of the oligonucleotides, the monolayer growth of antisense and control

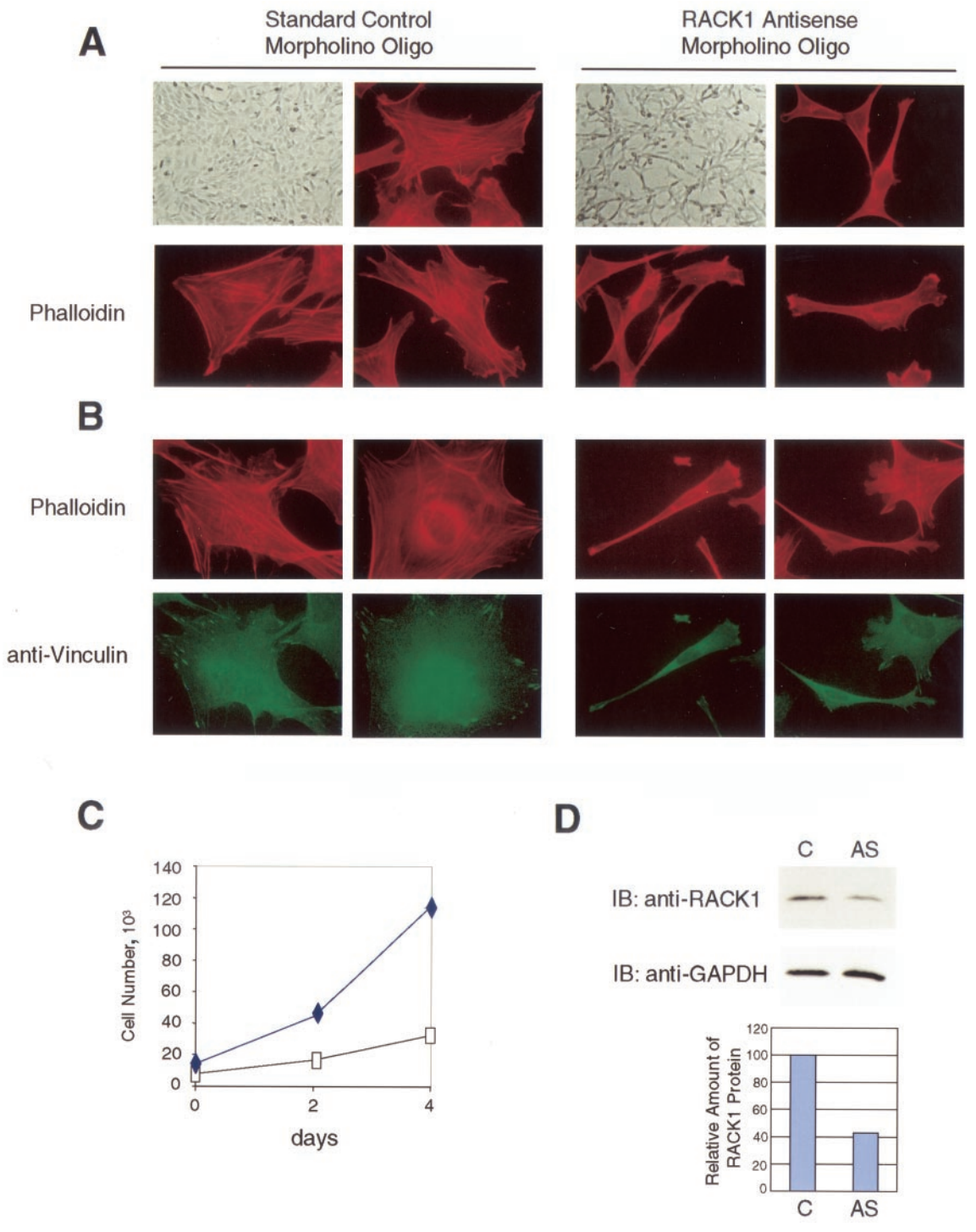

FIG. 10. Introduction of RACK1 antisense oligonucleotides suppresses cell spreading and attenuates IGF-I-dependent cell proliferation. (A) RACK1 antisense or control morpholino oligonucleotides were delivered to Swiss 3T3 cells as described in Materials and Methods. Photomicrographs under light microscopy (×40 magnification) show gross cell morphology 5 days after delivery of oligonucleotides. Cells were then fixed and stained with phalloidin-TRITC and visualized by fluorescence microscopy (upper right and lower panels). (B) The same cells were costained with phalloidin-TRITC (upper panels) and anti-vinculin Ab (lower panels) and examined by fluorescence microscopy. (C) At 2 weeks after introduction of oligonucleotides, Swiss 3T3 cells containing either control (♦) or antisense (□) oligonucleotides were plated sparsely at an equivalent cell density in medium containing 2% BCS and supplemental IGF-I at 100 ng/ml. Cells were counted in duplicate every other day to determine the growth rates. Growth in 2% BCS was analyzed in parallel cultures and confirmed the IGF-I-stimulated growth (data not shown). (D) At 2 weeks after the introduction of oligonucleotides, Swiss 3T3 cells were lysed and equivalent amounts of total cell lysate were separated by SDS-PAGE and immunoblotted (IB) with anti-RACK1 Ab (upper panel). Membranes were stripped and reprobed with anti-GAPDH Ab (lower panel). The relative amounts of RACK1 (normalized to GAPDH) in control and antisense oligonucleotide-containing cells were analyzed by using Image Tool software and are presented in the histogram.

cells was analyzed as described for RACK1-overexpressing cells. Proliferation of antisense cells was reduced by 34% after 2 days and by 50% after 4 days of growth relative to that of control cells (Fig. 10C). Suppression of cell spreading and monolayer growth in antisense cells was correlated with a reduction of the RACK1 protein level by 50 to 60% (Fig. 10D), suggesting that RACK1 plays an important role in cell spreading, formation of focal adhesions, and cell proliferation. The diminished ability of cells to spread when RACK1 expression was reduced by antisense oligonucleotide is consistent with the enhancement of cell spreading observed when RACK1 is overexpressed and thus strongly points to a role for endogenous RACK1 in mediating cell spreading.

DISCUSSION

IGF-IR mitogenic signaling functions are mediated by the major substrates Shc and IRS-I, which couple the receptor to the Ras/MAPK and PI3K pathways, respectively. However, it is likely that there are additional mediators that regulate other IGF-IR-mediated mitogenic signaling pathways. Using the kinase active cytoplasmic domain of IGF-IR in a yeast two-hybrid interaction trap to identify proteins that interact with IGF-IR, we identified RACK1, a WD repeat protein originally identified for its ability to bind activated PKCs. The interaction of RACK1 with IGF-IR appears to be specific since interaction was not observed with the closely related IR in yeast and mammalian cells, suggesting that RACK1 could be a mediator of IGF-IR functions that are distinct from those of IR. In both fibroblasts and epithelial cells, RACK1 interacted with IGF-IR in an IGF-I- and PMA-inducible manner, implicating the involvement of conventional and/or novel activated PKC isozymes in the association of RACK1 with IGF-IR. Consistent with this notion, RACK1 and IGF-IR were both associated with PKC after IGF-I treatment. This association was also stimulated by PMA, which again implicates the involvement of PKC activation in this process. Therefore, RACK1 is likely to play a role in regulating IGF-IR signaling pathways by a mechanism that involves the IGF-I-dependent association of RACK1 with PKC and IGF-IR, a process that may require the activation of PKC. Our study provides evidence for a novel role of RACK1 in the modulation of IGF-IR-mediated regulation of integrin-dependent signal transduction since our data demonstrate that overexpression of RACK1 leads to its subcellular redistribution, perturbation of IGF-I-mediated or IGF-IR-mediated integrin signaling, and dysregulation of G_1 cell cycle checkpoint proteins with resultant inhibition of cell growth.

The redistribution of RACK1 to the membrane fraction in fibroblast and epithelial cells that were transformed by certain PTK oncogenes supports a role for RACK1 in cell growth and transformation. This is particularly pertinent in view of the strongly suggested role of RACK1 as a scaffold protein interacting with a variety of molecules involved in different signaling pathways (see the introduction). In an effort to better understand the role of RACK1 in IGF-IR-mediated growth and transformation, we generated stable NIH 3T3 cell lines that overexpressed both IGF-IR and RACK1. Murine fibroblasts overexpressing IGF-IR have been shown to exhibit IGF-I-dependent cell transformation; i.e., they form colonies in soft agar in the presence of IGF-I (19, 32, 35, 49). We found that overexpression of RACK1 suppressed the IGF-I-stimulated anchorage-independent growth of NIH 3T3-IGFR cells. Furthermore, IGF-I-mediated growth of cells in monolayer cultures was inhibited when RACK1 was overexpressed, as well as when its expression was reduced by antisense oligonucleotides. Overexpression of RACK1 led to a redistribution of RACK1 from the cytoskeleton to other subcellular locations and also led to the constitutive association of RACK1 with IGF-IR, which was not further increased by IGF-I. The redistribution of the majority of RACK1 from the cytoskeletal fraction to the cytosolic fraction upon overexpression of exogenous RACK1 could result from the sequestration of a limiting factor in the cytosol by RACK1. This unknown factor presumably would be necessary for the stable association of RACK1 to the cytoskeleton. The depletion of RACK1 from the cytoskeleton could also result in diminished anchoring sites for the RACK1-interacting molecules cited above for recruitment to this subcellular location. The constitutive association of RACK1 with IGF-IR is consistent with the observation that the immediate IGF-IR-mediated signaling pathways, such as the MAPK and PI3K pathways, were not affected. Instead, the reduced cytoskeletal association opens up the possibility that IGF-I-induced signaling through integrin-associated molecules could be affected. Indeed, this is what was observed, and thus perturbation of IGF-I-dependent integrin signaling by overexpression of RACK1 could very well account for the observed inhibition of IGF-I-induced cell growth and transformation.

We demonstrated that RACK1 associated with β1 integrin in an IGF-I- and PMA-inducible manner, which suggests that RACK1 could act as a mediator of β1 integrin functions that involve IGF-IR and PKC. Furthermore, we also found that IGF-IR associated with β1 integrin in response to IGF-I or PMA, which raises the possibility that IGF-IR could regulate integrin-dependent functions through RACK1. IGF-I treatment resulted in the stimulation of β1 integrin-associated kinase activity, and when RACK1 was overexpressed this associated kinase activity was suppressed, indicating that RACK1 mediates an IGF-I-dependent β1 integrin signaling pathway, perhaps by coordinating the formation of an IGF-IR–RACK1–β1 integrin protein complex. Reduced cytoskeletal association of RACK1 upon its overexpression may underlie the perturbation of β1 integrin-associated protein kinase complex formation. FAK, PKC, ILK, and c-Src are among the protein kinases that have been shown to associate with β integrin (30). Identification of the RACK1-regulated integrin-associated kinase(s) is ongoing and will reveal a more precise role for RACK1 in coordinating IGFR and integrin functions.

Increasing evidence supports a role for IGF-IR in the regulation of focal adhesion molecules. FAK has been shown to become tyrosine phosphorylated and activated by IGF-IR in vitro (3). Additionally, $p130^{CAS}$ and paxillin, which associate with FAK and become tyrosine phosphorylated upon FAK activation, were shown to become tyrosine phosphorylated after IGF-I stimulation (12, 24). Our data indicate that overexpression of RACK1 in NIH 3T3-IGFR cells led to the suppression of IGF-I-dependent tyrosine phosphorylation of $p130^{CAS}$ and the association of $p130^{CAS}$ with Crk and other tyrosine-phosphorylated proteins, concomitant with an increase in the association of paxillin with Crk. Therefore, RACK1 appears to be involved in the IGF-IR-mediated reg-

ulation of focal adhesion proteins. The altered formation of Crk-specific protein complexes may be a consequence of the reduced integrin-associated kinase activity and is likely to alter downstream signaling.

Our results show that in RACK1-overexpressing NIH 3T3 cells maintained in complete medium, there exist higher levels of FAK and paxillin tyrosine phosphorylation compared to control cells (Fig. 4B). Yet, when those cells were serum starved and transiently stimulated with IGF-I, the IGF-I-inducible association of integrin with protein kinase(s) and association of Crk with $p130^{CAS}$ appeared to be diminished in the RACK1-overexpressing cells, whereas the association of Crk with paxillin was enhanced in RACK1-overexpressing cells (Fig. 7 and 8). The result in Fig. 4 reflects the overall effect of multiple growth factors and the sum of the effect of signaling functions altered due to RACK1 overexpression, whereas the result presented in Fig. 7 and 8 reflect the specific effects of RACK1 overexpression on IGF-I-induced integrin signaling functions. The mechanism by which overexpression of RACK1 causes the association of Crk to shift from $p130^{CAS}$ to paxillin is not clear. However, there are similar precedents in the switch of Crk binding from $p130^{CAS}$ to IRS-1 in response to insulin (54) and from CAS to Grb1 in cells transformed by a Tpr-Met oncogene (31). One possible explanation is that binding of paxillin to Crk is competitive with binding of $p130^{CAS}$ to Crk. Aternatively, binding of paxillin may induce a conformational change in Crk, to reducing its binding affinity toward $p130^{CAS}$.

Our immunofluorescence data demonstrated an increased number of stress fibers in RACK1-overexpressing cells, which was correlated with an increase in the spreading of these cells and an increase in the number of focal adhesions. These structural changes were associated with the increased tyrosine phosphorylation of FAK and paxillin, which has been shown to occur with increased cell spreading (41, 44, 45). Very recently, Buensuceso et al. (9) reported a similar observation of RACK1 overexpression in Chinese hamster ovary cells; these authors showed that RACK1 overexpression resulted in increased actin stress fibers and focal contacts and decreased migration and also noted that this effect of RACK1 required its binding to PKC. Nevertheless, these results were obtained by overexpression of RACK1. Our current data show that suppression of endogenous RACK1 expression by antisense oligonucleotides dramatically reduced cell spreading. Therefore, these data strongly point to a role for RACK1 in facilitating cell spreading through the regulation of the actin-based cytoskeleton and focal adhesions. Although cell spreading has been shown to be necessary for optimal cell cycle progression (28), we speculate that overexpression of RACK1 interferes with the dynamic regulation of focal adhesions, which would lead to a blunted response to β1 integrin-dependent mitogenic stimuli. This is supported by the inability of Crk to associate with $p130^{CAS}$ in response to IGF-I. Hence, the propagation of downstream signaling may be inhibited because of the inappropriate localization of Crk with paxillin instead of with $p130^{CAS}$. The absence or reduction of RACK1 in antisense cells would likely interfere and block signaling in an analogous manner.

Our analysis of cell cycle progression indicates that overexpression of RACK1 in NIH 3T3-IGFR cells caused a delay in IGF-I-dependent exit from G_0, progression through G_1, and/or entry into S at the G_1/S transition. Rb is believed to play an important role in controlling the transit of cells through the restriction point in G_1 (62). Hypophosphorylation of Rb in RACK1-overexpressing cells is consistent with a block in either of the latter two points in the cell cycle. The CKIs $p21^{Cip1/WAF1}$ and $p27^{Kip1}$ have been shown to inhibit the activities of the G_1- and S-phase cyclin/Cdk complexes that are responsible for phosphorylating and activating Rb, which is necessary for entry into S phase (52). Indeed, we found that the IGF-I-stimulated cyclin E-associated Cdk activity was significantly attenuated in cells overexpressing RACK1. Therefore, increased levels of $p21^{Cip1/WAF1}$ and $p27^{Kip1}$ are likely to inhibit cyclin/Cdk complexes, leading to the observed hypophosphorylation of Rb and inhibition of the G_1/S transition in RACK1-overexpressing cells. Since there were no alterations in the IGF-I-dependent activation of MAPK and PI3K pathways, RACK1 appears to regulate mitogenic signaling by an alternative mechanism. As discussed above, the reduced cytoskeletal localization of RACK1 may be partly responsible for causing the decreased association of Crk with $p130^{CAS}$ and, consequently, reduced integrin-mediated signaling. Although the exact mechanism is unclear, activation of integrin signaling has been shown to be necessary for the downregulation of $p21^{Cip1/WAF1}$ and $p27^{Kip1}$ CKIs and cell cycle pregression (26). Thus, interference with integrin-mediated signaling may account for the upregulation of $p21^{Cip1/WAF1}$ and $p27^{Kip1}$ and reduced cell proliferation. Although our results are consistent with a G_1/S delay in RACK1-overexpressing cells, we cannot rule out the possibility that a smaller population of cells is coming out of growth arrest.

While the effects of increasing and decreasing RACK1 levels consistently point to a role for endogenous RACK1 in facilitating cell spreading, the effects of manipulating RACK1 levels on cell proliferation are less consistent, since overexpression and antisense experiments both led to suppression of cell growth. Suppression of endogenous RACK1 expression would likely suppress the ability of RACK1 to carry out its cellular functions. Blockade of RACK1 expression by antisense oligonucleotides resulted in the suppression of IGF-I-dependent cell growth and thus suggests that RACK1 plays a positive role in IGF-I-mediated cell cycle progression and cell proliferation. The interpretation of the growth inhibition in RACK1-overexpressing cells is less straightforward since increased growth would be expected based on the suggested positive role of RACK1. However, RACK1 has been implicated to function as a scaffold protein, from both our study and those of others, and the overexpression of scaffold proteins has been reported to result in antagonism of endogenous function. For example, the scaffold protein JIP was initially shown to suppress JNK signaling when it was overexpressed alone but was later demonstrated to enhance JNK signaling when it was cooverexpressed with additional components of the MLK signaling pathway (21, 63). Sequestration of limiting components of the JNK pathway into separate protein complexes was suggested to be responsible for the inhibition caused by JIP overexpression (65). The overexpression and resulting redistribution in cellular localization of RACK1, which is likely to play a similar scaffolding role to enhance signaling at physiologic levels, could result in the sequestration or shifting of RACK1-binding molecules such as PKC or Src into separate and therefore nonfunctional signal-

ing complexes, i.e., in the cytosol rather than in the membrane or cytoskeletal fraction. The disruption of Crk complexes mentioned before further supports this idea. The function of RACK1 may depend on a strict equilibrium of its specific subcellular localization. Therefore, our data collectively point to a role for endogenous RACK1 to promote or facilitate cell cycle progression, cell proliferation, cell transformation, and cell spreading by IGF-IR and β1 integrin. Additionally, RACK1 may regulate the organization of the actin cytoskeleton either directly, as suggested by association of RACK1 with the subcellular cytoskeletal fraction, or indirectly through the coordination of focal adhesion proteins regulated by IGF-IR and β1 integrin.

The demonstrated interaction of RACK1 with multiple target molecules in response to IGF-I or PMA, along with the association of these molecules with each other, i.e., IGF-IR with PKC and β1 integrin, indicates that RACK1 may form multiprotein complexes in response to stimulation. Therefore, RACK1 may coordinate IGF-IR-mediated signaling by acting as a scaffold protein. In addition to the molecules described above, RACK1 has also been reported to associate with molecules including c-Src, a cyclic AMP phosphodiesterase, the beta chain of the interleukin-5/interleukin-3/granulocyte-macrophage colony-stimulating factor receptor, GABA type A receptors, PTPμ, and Stat1 (7, 13, 25, 38, 61, 64). While each of these molecules has been shown to be involved in signal transduction, the role of these molecules in mediating IGF-IR signaling pathways is not known. It remains to be determined whether those molecules interact with RACK1 in an IGF-I-dependent manner. Alternatively, RACK1 may perform scaffold functions for those signaling molecules that are separate from IGF-IR-mediated functions.

In conclusion, RACK1 is a newly described IGF-IR-interacting molecule which is involved in the regulation of IGF-IR-mediated cell growth, cell transformation, and integrin signaling. The precise mechanism by which RACK1 regulates these functions is unclear, but our current understanding supports a role for RACK1 in bridging cellular adhesion-mediated signaling with IGF-IR-regulated signaling. The interaction of RACK1 with an increasing number of molecules suggests that RACK1 may coordinate multiple functions within the cell by acting as a protein scaffold that could integrate a variety of extracellular stimuli. Further studies of RACK1 and its binding partners will undoubtedly define more precisely the role played by RACK1 in regulating cellular functions controlled by IGF-IR, integrins, and their relevant signaling molecules.

ACKNOWLEDGMENTS

We thank Roger Brent for providing the reagents for the yeast two-hybrid interaction trap and Andrew Chan for providing 3T3-RasV12 cells. We thank Wei Li for the initial identification of the IGF-1R-interacting protein, RACK1.

This work was supported by National Institutes of Health grants CA29339 and CA55054 (L.-H.W.). Partial support was provided by the Mount Sinai School of Medicine Medical Scientist Training Program, National Institute of General Medical Sciences grant T32GM07280 (U.H.).

REFERENCES

1. **Arbet-Engels, C., S. Tartare-Deckert, and W. Eckhart.** 1999. C-terminal Src kinase associates with ligand-stimulated insulin-like growth factor-I receptor. J. Biol. Chem. **274:**5422–5428.
2. **Assoian, R. K., and X. Zhu.** 1997. Cell anchorage and the cytoskeleton as partners in growth factor dependent cell cycle progression. Curr. Opin. Cell Biol. **9:**93–98.
3. **Baron, V., V. Calleja, P. Ferrari, F. Alengrin, and E. Van Obberghen.** 1998. $p125^{Fak}$ focal adhesion kinase is a substrate for the insulin and insulin-like growth factor-I tyrosine kinase receptors. J. Biol. Chem. **273:**7162–7168.
4. **Beitner-Johnson, D., and D. LeRoith.** 1995. Insulin-like growth factor-I stimulates tyrosine phosphorylation of endogenous c-Crk. J. Biol. Chem. **270:**5187–5190.
5. **Birge, R. B., J. E. Fajardo, C. Reichman, S. E. Shoelson, Z. Songyang, L. C. Cantley, and H. Hanafusa.** 1993. Identification and characterization of a high-affinity interaction between v-Crk and tyrosine-phosphorylated paxillin in CT10-transformed fibroblasts. Mol. Cell. Biol. **13:**4648–4656.
6. **Blenis, J.** 1993. Signal transduction via the MAP kinases: proceed at your own RSK. Proc. Natl. Acad. Sci. USA **90:**5889–5892.
7. **Brandon, N. J., J. M. Uren, J. T. Kittler, H. Wang, R. Olsen, P. J. Parker, and S. J. Moss.** 1999. Subunit-specific association of protein kinase C and the receptor for activated C kinase with GABA type A receptors. J. Neurosci. **19:**9228–9234.
8. **Brunet, A., A. Bonni, M. J. Zigmond, M. Z. Lin, P. Juo, L. S. Hu, M. J. Anderson, K. C. Arden, J. Blenis, and M. E. Greenberg.** 1999. Akt promotes cell survival by phosphorylating and inhibiting a Forkhead transcription factor. Cell **96:**857–868.
9. **Buensuceso, C. S., D. Woodside, J. L. Huff, G. E. Plopper, and T. E. O'Toole.** 2001. The WD protein Rack1 mediates protein kinase C and integrin-dependent cell migration. J. Cell Sci. **114:**1691–1698.
10. **Cantley, L. C., K. R. Auger, C. Carpenter, B. Duckworth, A. Granziani, R. Kapeller, and S. Soltoff.** 1991. Oncogene and signal transduction. Cell **64:**281–302.
11. **Cary, L. A., and J. L. Guan.** 1999. Focal adhesion kinase in integrin-mediated signaling. Front. Biosci. **4:**D102–D113.
12. **Casamassima, A., and E. Rozengurt.** 1998. Insulin-like growth factor I stimulates tyrosine phosphorylation of $p130^{Cas}$, focal adhesion kinase, and paxillin. Role of phosphatidylinositol 3′-kinase and formation of a $p130^{Cas}$-Crk complex. J. Biol. Chem. **273:**26149–26156.
13. **Chang, B. Y., K. B. Conroy, E. M. Machleder, and C. A. Cartwright.** 1998. RACK1, a receptor for activated C kinase and a homolog of the beta subunit of G proteins, inhibits activity of src tyrosine kinases and growth of NIH 3T3 cells. Mol. Cell. Biol. **18:**3245–3256.
14. **Chang, B. Y., M. Chiang, and C. A. Cartwright.** 2001. The interaction of Src and RACK1 is enhanced by activation of protein kinase C and tyrosine phosphorylation of RACK1. J. Biol. Chem. **276:**20346–20356.
15. **Cheatham, B., C. J. Vlahos, L. Cheatham, L. Wang, J. Blenis, and C. R. Kahn.** 1994. Phosphatidylinositol 3-kinase activation is required for insulin stimulation of pp70 S6 kinase, DNA synthesis, and glucose transporter translocation. Mol. Cell. Biol. **14:**4902–4911.
16. **Chen, J., H. B. Sadowski, R. A. Kohanski, and L.-H. Wang.** 1997. Stat5 is a physiological substrate of the insulin receptor. Proc. Natl. Acad. Sci. USA **94:**2295–2300.
17. **Craparo, A., R. Freund, and T. A. Gustafson.** 1997. 14–3-3ε interacts with the insulin-like growth factor I receptor and insulin receptor substrate I in a phosphoserine-dependent manner. J. Biol. Chem. **272:**11663–11669.
18. **Datta, S. R., H. Dudek, X. Tao, S. Masters, H. Fu, Y. Gotoh, and M. E. Greenberg.** 1997. Akt phosphorylation of BAD couples survival signals to the cell-intrinsic death machinery. Cell **91:**231–241.
19. **Davis, R. J.** 1993. The mitogen-activated protein kinase signal transduction pathway. J. Biol. Chem. **268:**14553–14556.
20. **Dey, B. R., S. L. Spence, P. Nissley, and R. W. Furlanetto.** 1998. Interaction of human suppressor of cytokine signaling (SOCS)-2 with the insulin-like growth factor-I receptor. J. Biol. Chem. **273:**24095–24101.
21. **Dickens, M., J. S. Rogers, J. Cavanagh, A. Raitano, Z. Xia, J. R. Halpern, M. E. Greenberg, C. L. Sawyers, and R. J. Davis.** 1997. A cytoplasmic inhibitor of the JNK signal transduction pathway. Science **277:**693–696.
22. **Feldman, E. L., K. A. Sullivan, B. Kim, and J. W. Russell.** 1997. Insulin-like growth factors regulate neuronal differentiation and survival. Neurobiol. Dis. **4:**201–214.
23. **Fields, S., and O. Song.** 1989. A novel genetic system to detect protein-protein interactions. Nature **340:**245–246.
24. **Fujita, T., H. Maegawa, A. Kashiwagi, H Hirai, and R. Kikkawa.** 1998. Opposite regulation of tyrosine-phosphorylation of $p130^{Cas}$ by insulin and insulin-like growth factor I. J. Biochem. **124:**1111–1116.
25. **Geijsen, N., M. Spaargaren, J. A. Raaijmakers, J. W. Lammers, L. Koenderman, and P. J. Coffer.** 1999. Association of RACK1 and PKCβ with the common beta-chain of the IL-5/IL-3/GM-CSF receptor. Oncogene **18:**5126–5130.
26. **Giancotti, F. G., and E. Ruoslahti.** 1999. Integrin signaling. Science **285:**1028–1032.
27. **Gustafson, T. A., W. He, A. Craparo, C. D. Schaub, and T. J. O'Neill.** 1995. Phosphotyrosine-dependent interaction of SHC and insulin receptor substrate 1 with the NPEY motif of the insulin receptor via a novel non-SH2 domain. Mol. Cell. Biol. **15:**2500–2508.
28. **Huang, S., C. S. Chen, and D. E. Ingber.** 1998. Control of cyclin D1, $p27^{Kip1}$,

and cell cycle progression in human capillary endothelial cells by cell shape and cytoskeletal tension. Mol. Biol. Cell **9:**3179–3193.
29. **Kaleko, M., W. J. Rutter, and A. D. Miller.** 1990. Overexpression of the human insulinlike growth factor I receptor promotes ligand-dependent neoplastic transformation. Mol. Cell. Biol. **10:**464–473.
30. **Kumar, C. C.** 1998. Signaling by integrin receptors. Oncogene **17:**1365–1373.
31. **Lamorte, L., D. M. Kamikura, and M. Park.** 2000. A switch from p130Cas/Crk to Gab1/Crk signaling correlates with anchorage independent growth and JNK activation in cells transformed by the Met receptor oncoprotein. Oncogene **19:**5973–5981.
32. **Li, W., Y. X. Jiang, J. Zhang, L. Soon, L. Flechner, V. Kapoor, J. H. Pierce, and L.-H. Wang.** 1998. Protein kinase C-delta is an important signaling molecule in insulin-like growth factor I receptor-mediated cell transformation. Mol. Cell. Biol. **18:**5888–5898.
33. **Liliental, J., and D. D. Chang.** 1998. Rack1, a receptor for activated protein kinase C, interacts with integrin beta subunit. J. Biol. Chem. **273:**2379–2383.
34. **Liu, D., C. S. Zong, and L.-H. Wang.** 1993. Distinctive effects of the carboxyl-terminal sequence of the insulin-like growth factor I receptor on its signaling functions. J. Virol. **67:**6835–6840.
35. **Liu, D., W. J. Rutter, and L.-H. Wang.** 1992. Enhancement of transforming potential of human insulin-like growth factor 1 receptor by N-terminal truncation and fusion to avian sarcoma virus UR2 gag sequence. J. Virol. **66:** 374–385.
36. **McLeod, M., B. Shor, A. Caporaso, W. Wang, H. Chen, and L. Hu.** 2000. Cpc2, a fission yeast homologue of mammalian RACK1 protein, interacts with Ran1 (Pat1) kinase to regulate cell cycle progression and meiotic. Mol. Cell. Biol. **20:**4016–4027.
37. **Morrione, A., B. Valentinis, S. Li, J. Y. Ooi, B. Margolis, and R. Baserga.** 1996. Grb10: a new substrate of the insulin-like growth factor I receptor. Cancer Res. **56:**3165–3167.
38. **Mourton, T., C. B. Hellberg, S. M. Burden-Gulley, J. Hinman, A. Rhee, and S. M. Brady-Kalnay.** 2001. The PTPμ protein-tyrosine phosphatase binds and recruits the scaffolding protein RACK1 to cell-cell contacts. J. Biol. Chem. **276:**14896–14898.
39. **Neckameyer, W. S., and L.-H. Wang.** 1984. Molecular cloning and characterization of avian sarcoma virus UR2 and comparison of its transforming sequence with those of other avian sarcoma viruses. J. Virol. **50:**914–921.
40. **Nguyen, K. T., W. J. Wang, J. L. Chan, and L.-H. Wang.** 2000. Differential requirements of the MAP kinase and PI3 kinase signaling pathways in Src-versus insulin and IGF-1 receptor-induced growth and transformation of rat intestinal epithelial cells. Oncogene **19:**5385–5397.
41. **Nishiya, N., K. Tachibana, M. Shibanuma, J. I. Mashimo, and K. Nose.** 2001. Hic-5-reduced cell spreading on fibronectin: competitive effects between paxillin and Hic-5 through interaction with focal adhesion kinase. Mol. Cell. Biol. **21:**5332–5345.
42. **Ogawa, W., T. Matozaki, and M. Kasuga.** 1998. Role of binding proteins to IRS-1 in insulin signalling. Mol. Cell. Biochem. **182:**13–22.
43. **Poon, B., D. Dixon, L. Ellis, R. A. Roth, W. J. Rutter, and L-. H. Wang.** 1991. Molecular basis of the activation of the tumorigenic potential of Gag-insulin receptor chimeras. Proc. Natl. Acad. Sci. USA **88:**877–881.
44. **Richardson, A., R. K. Malik, J. D. Hildebrand, and T. Parsons.** 1997. Inhibition of cell spreading by expression of the C-terminal domain of focal adhesion kinase (FAK) is rescued by coexpression of Src or catalytically inactive FAK: a role for paxillin tyrosine phosphorylation. Mol. Cell. Biol. **17:**6906–6914.
45. **Richardson, A., and T. Parsons.** 1996. A mechanism for regulation of the adhesion-associated protein tyrosine kinase $pp125^{FAK}$. Nature **380:**538–540.
46. **Ron, D., C. H. Chen, J. Caldwell, L. Jamieson, E. Orr, and D. Mochly-Rosen.** 1994. Cloning of an intracellular receptor for protein kinase C: a homolog of the beta subunit of G proteins. Proc. Natl. Acad. Sci. USA **91:**839–843.
47. **Ron, D., J. Luo, and D. Mochly-Rosen.** 1995. C2 region-derived peptides inhibit translocation and function of beta protein kinase C in vivo. J. Biol. Chem. **270:**24180–24184.
48. **Ron, D., Z. Jiang, L. Yao, A. Vagts, I. Diamond, and A. Gordon.** 1999. Coordinated movement of RACK1 with activated βIIPKC. J. Biol. Chem. **274:**27039–27046.
49. **Rubin, R., and R. Baserga.** 1995. Insulin-like growth factor-I receptor, its role in cell proliferation, apoptosis, and tumorigenicity. Lab. Investig. **73:** 311–331.
50. **Seely, B. L., D. R. Reichart, P. A. Staubs, B. H. Jhun, D. Hsu, H. Maegawa, K. L. Milarski, A. R. Saltiel, and J. M. Olefsky.** 1995. Localization of the insulin-like growth factor I receptor binding sites for the SH2 domain proteins p85, Syp, and GTPase activating protein. J. Biol. Chem. **270:**19151–19157.
51. **Sepp-Lorenzino, L.** 1998. Structure and function of the insulin-like growth factor I receptor. Breast Cancer Res. Treat. **47:**235–253.
52. **Sherr, C. J., and J. M. Roberts.** 1999. CDK inhibitors: positive and negative regulators of G_1-phase progression. Genes. Dev. **13:**1501–1512.
53. **Skolnik, E. Y., A. Batzer, N. Li, C. H. Lee, E. Lowenstein, M. Mohammadi, B. Margolis, and J. Schlessinger.** 1993. The function of GRB2 in linking the insulin receptor to Ras signaling pathways. Science **260:**1953–1955.
54. **Sorokin, A., and E. Reed.** 1998. Insulin stimulates the tyrosine dephosphorylation of docking protein $p130^{cas}$ (Crk-associated substrate), promoting the switch of the adaptor protein Crk from $p130^{cas}$ to newly phosphorylated insulin receptor substrate-1. Biochem. J. **334:**595–600.
55. **Stewart, C. E., and P. Rotwein.** 1996. Growth, differentiation, and survival: multiple physiological functions for insulin-like growth factors. Physiol. Rev. **76:**1005–1026.
56. **Summerton, J.** 1999. Morpholino antisense oligomers: the case for an RNase H-independent structural type. Biochim. Biophys. Acta **1489:**141–158.
57. **Sun, X. J., D. L. Crimmins, M. G. Myers, Jr., M. Miralpeix, and M. F. White.** 1993. Pleiotropic insulin signals are engaged by multisite phosphorylation of IRS-1. Mol. Cell. Biol. **13:**7418–7428.
58. **Sun, X. J., P. Rothenberg, C. R. Kahn, J. M. Backer, E. Araki, P. A. Wilden, D. A. Cahill, B. J. Goldstein, and M. F. White.** 1991. Structure of the insulin receptor substrate IRS-1 defines a unique signal transduction protein. Nature **352:**73–77.
59. **Tartare-Deckert, S., J. Murdaca, D. Sawka-Verhelle, K. H. Holt, J. E. Pessin, and E. Van Obberghen.** 1996. Interaction of the molecular weight 85K regulatory subunit of the phosphatidylinositol 3-kinase with the insulin receptor and the insulin-like growth factor-1 (IGF-I) receptor: comparative study using the yeast two-hybrid system. Endocrinology **137:**1019–1024.
60. **Uddin, S., A. Yetter, S. Katzav, C. Hofmann, M. F. White, and L. C. Platanias.** 1996. Insulin-like growth factor-1 induces rapid tyrosine phosphorylation of the vav proto-oncogene product. Exp. Hematol. **24:**622–627.
61. **Usacheva, A., R. Smith, R. Minshall, G. Baida, S. Seng, E. Croze, and O. Colamonici.** 2001. The WD motif-containing protein receptor for activated protein kinase C (RACK1) is required for recruitment and activation of signal transducer and activator of transcription 1 through the type I interferon receptor. J. Biol. Chem. **276:**22948–22953.
62. **Weinberg, R. A.** 1995. The retinoblastoma protein and cell cycle control. Cell **81:**323–330.
63. **Whitmarsh, A. J., J. Cavanagh, C. Tournier, J. Yasuda, and R. J. Davis.** 1998. A mammalian scaffold complex that selectively mediates MAP kinase activation. Science **281:**1671–1674.
64. **Yarwood, S. J., M. R. Steele, G. Scotland, M. D. Houslay, and G. B. Bolger.** 1999. The RACK1 signaling scaffold protein selectively interacts with the cAMP-specific phosphodiesterase PDE4D5 isoform. J. Biol. Chem. **274:** 14909–14917.
65. **Yasuda, J., A. J. Whitmarsh, J. Cavanagh, M. Sharma, and R. J. Davis.** 1999. The JIP group of mitogen-activated protein kinase scaffold proteins. Mol. Cell. Biol. **19:**7245–7254.
66. **Zeng, L., P. Sachdev, L. Yan, J. L. Chan, T. Trenkle, M. McClelland, J. Welsh, and L.-H. Wang.** 2000. Vav3 mediates receptor protein tyrosine kinase signaling, regulates GTPase activity, modulates cell morphology, and induces cell transformation. Mol. Cell. Biol. **20:**9212–9224.
67. **Zervos, A. S., J. Gyuris, and R. Brent.** 1993. Mxi1, a protein that specifically interacts with Max to bind Myc-Max recognition sites. Cell **72:**223–232.
68. **Zong, C. S., J. Chan, D. E. Levy, C. Horvath, H. B. Sadowski, and L.-H. Wang.** 2000. Mechanism of STAT3 activation by insulin-like growth factor I receptor. J. Biol. Chem. **275:**15099–15105.
69. **Zong, C. S., J. L. Chan, S. K. Yang, and L.-H. Wang.** 1997. Mutations of Ros differentially effecting signal transduction pathways leading to cell growth versus transformation. J. Biol. Chem. **272:**1500–1506.